NAL PROPOSAL No. 0052

Correspondent: H. Weisberg
Department of Physics
University of Pennsylvani
Philadelphia, Pa. 19104

FTS/Off-net: 215-597-3311
594-8141

A PROPOSAL TO STUDY PARTICLE PRODUCTION SPECTRA AND MULTIPLICITIES IN HIGH ENERGY HADRON-HADRON COLLISIONS, AND FOR A BEAM SURVEY AND QUARK SEARCH

E. W. Beier, D. L. Kreinick, H. Weisberg
University of Pennsylvania

June 15, 1970

UNIVERSITY of PENNSYLVANIA
PHILADELPHIA 19104

The College
DEPARTMENT OF PHYSICS

A PROPOSAL TO STUDY PARTICLE PRODUCTION SPECTRA AND MULTIPLICITIES IN HIGH ENERGY HADRON-HADRON COLLISIONS, AND FOR A BEAM SURVEY AND QUARK SEARCH

We propose an experimental study at the new 500 Gev accelerator of the differential cross-section for particle production in hadron-hadron collisions. The projectile, and the observed single particle, will range over all combinations of positive and negative π, K and p, with momenta extending up to the highest available. Enough of the secondary particle momentum range will be covered to permit us to determine by integration the multiplicity of the produced particle.

Single particles will be detected in a simple spectrometer consisting of wire chambers and a small bending magnet. The configuration of the spectrometer components will be variable so that the overall spectrometer length can be kept proportional to the secondary momentum. The momentum resolution $\delta P/P = \pm 0.8\%$ and the invariant phase space acceptance $P^2 d\Omega dP/E = 1.3 \times 10^{-3} (\text{Gev/c})^2$ will then be the same at all momenta. Particle identification will be by means of threshold Čerenkov counters, with 10^4: 1 rejection up to at least 250 Gev/c.

Our experimental arrangement is thought to be simple and yet powerful, and we propose its use initially with incident protons and a nuclear target for a beam survey and quark search. Subsequent measurements will be carried out with a hydrogen target in a high intensity secondary beam.

Experimenters: Eugene W. Beier, David L. Kreinick and Howard Weisberg

Date: June 15, 1970

Correspondent: Howard Weisberg

TABLE OF CONTENTS

1. INTRODUCTION

Multiparticle production plays a dominating role in hadron-hadron scattering at high energies. The detailed experimental study of the multiparticle channels becomes exceedingly difficult as the energy increases, especially because of the problem of missing neutrals. Furthermore, even if one had detailed information, its theoretical understanding would be difficult because of the problem of organizing the vast amount of data that would be involved. These considerations lead one to hope that, by studying simple features of high energy scattering, some groundwork for theoretical understanding can be laid. Feynman[1] and others have emphasized this line of argument.

The simplest features of inelastic scattering are:

(1) total cross sections

(2) multiplicities

(3) single particle momentum distributions

(4) two particle correlation functions

Each of these can be studied as a function of energy and particle type. Our experiment is intended to be a rather comprehensive first look at (2) and (3) in a newly accessible energy range.

Specifically we propose to measure the differential cross section for the production of particle c in the reaction ab→cd,

$$\frac{d\sigma}{d^3\underline{P}^*}(ab\to c) \equiv \sum_d \frac{d\sigma}{d^3\underline{P}^*}(ab\to cd)$$

where a, c = p, $\bar{p}$, $\pi^{\pm}$, and $K^{\pm}$, b = p, d ranges over all available states and is not detected in our experiment, and $\underline{P}^*$ is the cm

momentum of c.

We shall measure the dependence of these distributions on longitudinal c.m. momentum $P_{||}{}^*$, transverse momentum $\underline{P}_T$, incoming c.m. momentum P_a^* and on the identities of particles a and c Furthermore our measurements shall cover a wide enough range of $\underline{P}^*$ to permit us to determine the average multiplicity $\bar{n}$ of particle c from the integral

$$\bar{n}\ \sigma = \int \frac{d\sigma}{d^3\underline{P}^*}\ d^3\underline{P}^*.$$

where σ is the total cross section, which will be known from other experiments.

This experimental approach will be particularly fruitful if it should turn out that multiparticle production has some of the features of a rather random, incoherent process, in the spirit of the original Fermi statistical model[2], or of current ideas of limiting fragmentation[3] and partons[1,4], as discussed below in Section 2.

Recently there has been much interest in studies of the process of inelastic electron scattering, because of the observation that, as the momentum transfer increases, the "bumps" die away while the "background" holds up, and that an apparent scaling law holds.[5] For hadron-hadron scattering, the analogous facts are that as the energy goes up, cross sections for specific channels fall off with Regge s^α behavior, and that there is an apparent tendency to approach limiting distributions for the remaining, largely inelastic, processes. These facts suggest an analogous interest in hadron-hadron inelastic

scattering studies of the type proposed here.

Finally, we believe that there is merit in studying single particle production spectra that is independent of any particular theoretical ideas that one may be testing. These distributions are simple, basic, and easily acessible experimentally. The richness of the range of information available suggests that the data may well turn out to have significance that can only be seen a posteriori.

This type of experiment seems to have been somewhat neglected in the past, with a few notable exceptions of particle production in pp collisions[6] and one recent result on longitudinal moments of negatives in π^-p collisions[7].

In Section 2 we review theoretical ideas about inelastic hadron-hadron scattering. In Section 3 we describe the experimental apparatus, a spectrometer with length proportional to the momentum measured. This variable length spectrometer enables us to obtain a momentum resolution and acceptance which are independent of momentum and it covers the entire kinematic range of the distribution we are measuring.

In Section 4, we discuss the kinematics of particle production, to determine what range of laboratory momenta and angles must be covered. In Section 5, we give a simple estimate of the counting rates, and a determination of the momentum and angle acceptance needed to achieve a given experimental sensitivity.

In our experimental design, there is a limit to the maximum beam intensity that can be used. This limit is essentially set by the requirement that the singles rates (counting rate integrated over all momenta) in the counters and wire chambers not be too great. In Section 6 we use the counting rate analysis of Section 5 to estimate the maximum beam rate that we can handle; this limit turns out to be independent of the spectrometer length, and is around 10^8 particles per second.

Particle identification is discussed in Section 7. Here again a variable length design is used. The needed threshold Čerenkov counter length is obtained by bolting various lengths of tubing together, with a phototube and mirror module on the end. The total mass of radiator is the same at all momenta. However, the length needed goes as the square of the momentum, so our simple scaling property breaks down and there is a momentum at which the entire available spectrometer length is filled with Čerenkov counters.

The detailed performance of the spectrometer is discussed in Section 8. In particular, the dependence of the acceptance on momentum and the effect of multiple scattering on the momentum resolution are presented. Also the momentum range of the threshold Cerenkov counters is compared to the momentum bite of the spectrometer.

In Section 9 we propose that our experiment be set up initially with a proton beam to carry out a beam survey and quark search. Section 10 gives an estimate of the running time needed, Section 11 discusses beam requirements and Section 12 discusses equipment and manpower.

2. THEORIES OF HIGH ENERGY HADRON-HADRON INELASTIC SCATTERING

In the Fermi statistical model[2], the energy of the incident particles is dumped into a small region whose size is of the order of the incident particle size; this energy then escapes, in the form of hadronic matter, with equal probability into all available channels. It is well known that this model seriously disagrees with observation. In particular it fails to account for the fact that transverse momenta are always limited to small values, even at high bombarding energy. Nonetheless the model, which was formulated before there was quantitative data on particle production, retains its appeal. It provides one with the simple picture of the collision of two extended blobs of hadronic matter with rather well defined sizes, and to this day it provides bump hunting experimental physicists with a convenient parameterization for the vast expanses of inelastic background which, at high energies, underlie the progressively tinier and tinier bumps that they find.

Hagedorn[8] has modified the statistical model to get agreement with existing observations, by invoking a maximum temperature for nuclear matter and by considering particles emanating from two outgoing "fireballs" associated with the incoming hadrons.

Yang[3] has emphasized the picture of hadrons as extended objects that are rather transparent to each other. This picture leads to the hypothesis of limiting fragmentation, by the following argument. Viewed in the rest system of the target, the projectile is a pancake

shaped object passing by with essentially the velocity of light. At high energies, some or all of the matter in the target might then be expected to emerge in a way that, at high bombarding energy, no longer depends on the energy. Similarly there would be emerging particles that are fragments of the projectile, and have limiting momentum distributions in the projectile rest frame. Existing experimental data tend to support this hypothesis. The increasing multiplicity at high energies would then correspond, at least in part, to more and more of the limiting distribution becoming kinematically accessible.

Feynman[2] reaches essentially the same conclusion about limiting distributions by arguments based on the picture that hadrons are made up of point-like constituents (partons) whose interactions are similar to those of simple field theory. These arguments are conveniently stated in frames in which the incoming particles have large momentum, and in particular in the c.m. frame. The incoming hadrons are made up virtually of constituents, each characterized by x, its fraction of the incoming longitudinal momentum and by P_T, its transverse momentum, which is hypothesized to be small. Simple quantum mechanical arguments then suggest that in the collision only patrons of "wee" x - those having longitudinal momentum in the c.m. of ≤ 1 Gev/c, can be exchanged. In that case, the momentum distribution of the outgoing constituents and hence, after appropriate final state interactions, of the outgoing particles observed in the lab, will reflect that of the constituents coming in.

The limiting fragmentation idea translates for the single particle momentum distributions in the c.m. into the statement that

$$\frac{d\sigma}{dx d^2 p_T} = f(x, p_T)$$

where f does not depend on the incident energy. Particles of definite negative x correspond, by Lorentz transformation, to particles of definite momentum in the target frame, while particles of definite positive x correspond to particles of definite momentum in the projectile rest frame, in the limit of high incoming energies.

One then will have target independence: the momentum distribution of the fragments of the projectile ($x>0$) will depend only on the identity of the projectile and not of the target, and conversely for the secondaries with $x<0$. A further prediction is that transverse momenta will be limited, independent of energy.

A hint that the parton model may have some validity comes from inelastic electron scattering, which behavior can be explained by elastic scattering of the electrons from point partons having a fraction $x = Q^2/2M\nu$ of the total incoming proton momentum.[5] In fact if the parton model is correct, the observed cross section for a given x is a measure of the probability of finding a parton with longitudinal fraction x in the incoming hadron. According to the observed cross sections, this probability goes as $1/x$.

For hadron-hadron collisions, the increase with energy of the multiplicity comes from the fact that more and more of the region of

small x becomes available. At any finite energy the 1/x distribution would extend only down to the "wee" region rather than to zero. The multiplicity is equal to the integral of the longitudinal momentum distribution over all x, divided by the total cross section. If the total cross section is constant with energy, then by integrating 1/x down to x = [1 Gev/incident energy], we find a logarithmic dependence of the multiplicity on energy.

A number of the experimental predictions mentioned above, such as limited transverse momentum and inelasticities, target independence, logarithmic increase of multiplicity with energy and 1/x longitudinal momentum dependence for small x, also come from multiperipheral and multi-Regge models.[9]

Figure 1 shows some experimental information on single particle longitudinal momentum distributions. The data on $pp \to p$ and $pp \to \pi^-$ were obtained by numerical integration of the strong-focussing single-arm spectrometer data of Allaby et al[6]. The other two curves were obtained from new bubble chamber data of Elbert and Erwin[7] on the longitudinal momentum dependence of negative particles from 25 Gev π^-p collisions, in which all negative particles are assumed to be π^-'s. Their data for positive longitudinal momentum are presented as π^-p$\to\pi^-$ while their data for negative longitudinal momentum have been reflected about $P_{||} = 0$ and labeled $p\pi^- \to \pi^-$. The measured values of $\frac{d\sigma}{dx}$ have in each case been multiplied by a factor of $\frac{x}{\sigma}$ where the σ factor is included to get a dimensionless quantity, and

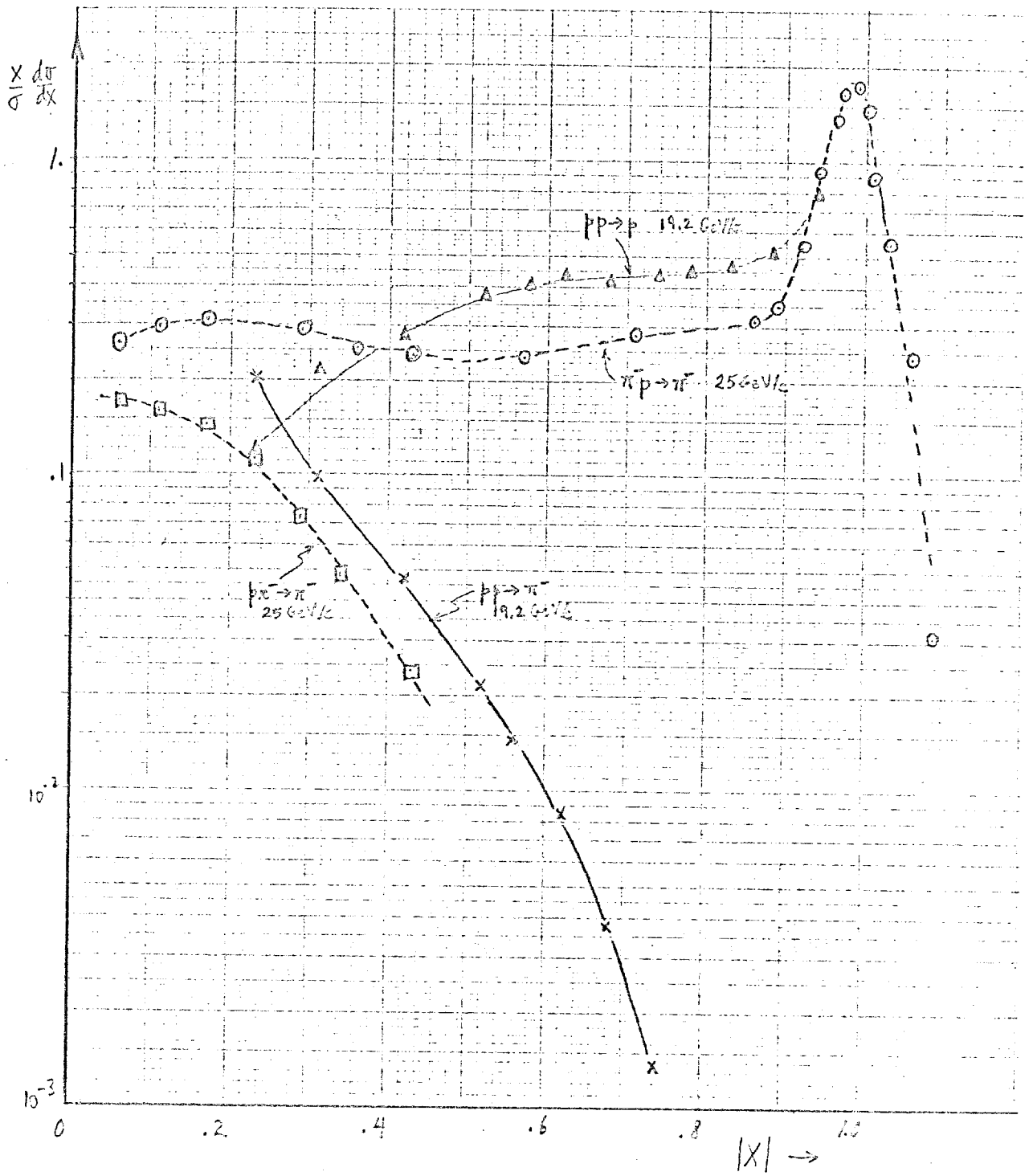

FIGURE 1. Experimentally observed values of $\frac{1}{\sigma} \times \frac{d\sigma}{dx}$. The curves for $\pi^- p \to \pi^-$ and $p\pi^- \to \pi^-$ were obtained from the data of Reference 7 as discussed in the text. The $p\pi^- \to \pi^-$ curve was obtained from the $\pi^- p \to \pi^-$ data for $x<0$ by reflection about $x=0$. The curves for $pp \to p$ and $pp \to \pi^-$ were obtained from the data of Reference 6 by numerical integration over the transverse momenta.

the x factor is included so that a 1/x longitudinal momentum dependence would appear as a tendency for the data to approach a constant for small, but not wee, x. The similarity of the $pp \to \pi^- X$ and $p\pi^- \to \pi^- X$ curves suggests that some sort of target independence may indeed hold.

3. THE EXPERIMENTAL ARRANGEMENT.

Our experimental design is based on the following ideas:

(1) Transverse momenta in hadron-hadron collisions are limited to $\lesssim$ 1 Gev/c. Therefore in order to cover the entire range of x from -1 to +1, we need to cover essentially two regions of laboratory momentum and angle, a small angle "forward region" covering a wide momentum range, and a "backward" region covering all laboratory angles but with momentum limited to $\lesssim$ 1 Gev/c.

(2) A momentum resolution of the order of 1% is more than adequate for the phenomena we wish to study. Since with careful design the transverse momentum from multiple scattering can be kept to a few Mev/c, the analyzing magnet need only have a transverse momentum impulse of a few hundreds of Mev/c.

(3) The acceptance $P^2 d\Omega \frac{dP}{E}$ in invariant phase space should be roughly constant over the entire range covered.

(4) The instantaneous beam rate in a secondary beam at NAL will be $\sim 10^8$ particles per second. Since we can therefore use detectors which view the target directly, we do not need to use a strong-focussing spectrometer. This situation is unlike the one at SLAC, where the instantaneous beam rate in the external beam is $\sim 10^9$ times greater.

Based on these considerations, we have designed a variable

configuration single-arm spectrometer, consisting of wire chambers and a small magnet. The "forward" region is covered by a sequence of configurations of different lengths, ranging from 200 meters down to 3.1 meters, covering momenta from 160 Gev/c down to 1.25 Gev/c, at transverse momenta from 0.13 Gev/c up to 3.5 Gev/c. The "backward" region is covered by a small fixed length spectrometer pivoted around the target.

It is expected that each configuration changeover can be carried out in a few hours; simple optical techniques will be used for alignment. The schedule of data taking will be arranged so that we take a complete set of data at each spectrometer configuration before changing lengths; there will be 8 configurations.

Figure 2a is a sketch of the layout for the "forward" data taking. The beam, which contains an unseparated mixture of pions, kaons and protons or antiprotons, is incident on a liquid hydrogen target. Cerenkov counters in the beam (not shown) identify the incident particles. The unscattered beam travels to a distant shielded beam dump. Scattered particles are detected, and their trajectories determined, in wire chambers $W_{1,2,3}$. Momentum analysis is provided by magnet M_1, and the trajectories after the magnet are determined by wire chambers $W_{4,5,6}$. Threshold Cerenkov counters $\check{C}_1$, $\check{C}_2$, and $\check{C}_3$ determine whether the scattered particle is a proton, a kaon or a light particle (pion,

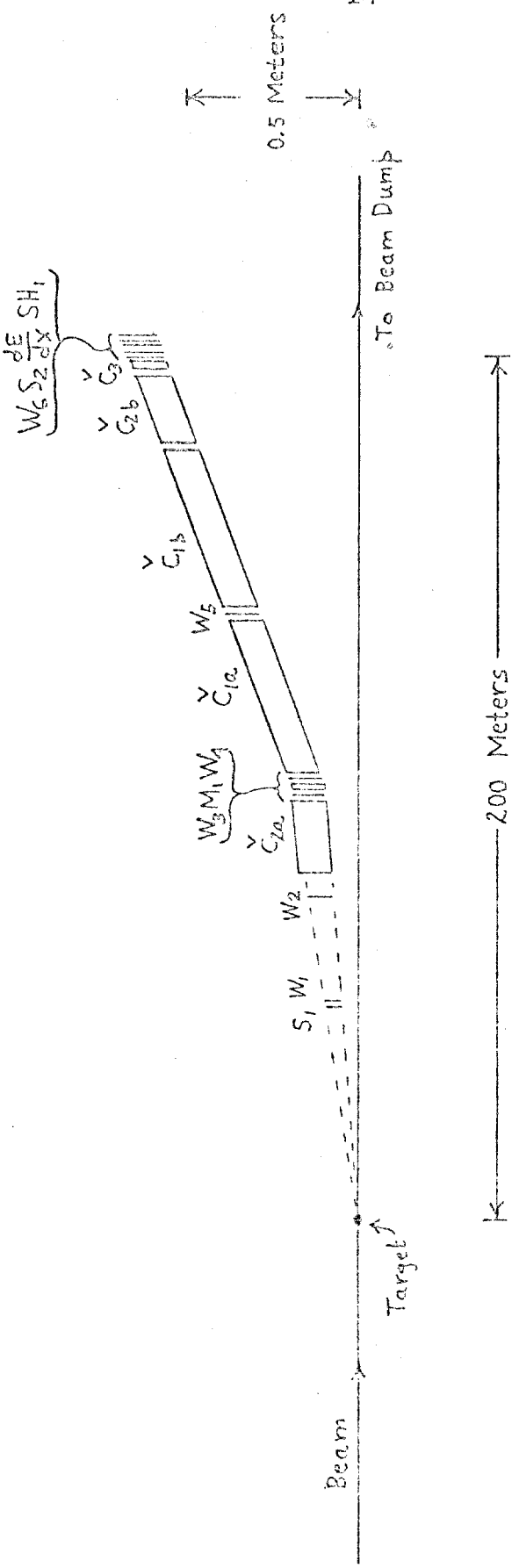

Figure 2a. A sketch of the layout of the "forward" spectrometer configuration, as seen from above. The dimensions shown are for the momentum band 80-160 Gev/c. The scale for any other momentum band is obtained by scaling the longitudinal distances linearly with momentum.

muon or electron). The event trigger is basically a coincidence between scintillation counters S_1 and S_2 and a Čerenkov counter. Energy loss counters ("dE/dX" in the figure) identify particles of non-integral charge, quarks in particular; shower counter SH_1 identifies electrons. Muons are distinguished from pions by the requirement that they traverse several interaction lengths of matter.

The needed coverage in transverse momentum is obtained by moving the spectrometer components on rails transverse to the beam. The motion will be remote controlled so that changes can be effected in a very short time. Since the scattering angle is small, transverse motion is just as good as motion along arcs centered on the target. In order to reach a transverse momentum of 3.5 Gev/c, the experimental area has to extend out to one side of beam center line a distance of

$$\frac{3.5 \text{ Gev/c}}{160 \text{ Gev/c}} \times 200 \text{ meters} - 0.5 \text{ Meters} = 3.9 \text{ meters}$$

The saving of 0.5 meters comes from bending toward rather than away from the beam line when we are at large angles.

There is an alternative way to vary the scattering angle, which is to use deflecting magnets and keep the spectrometer fixed. A magnet just downstream of the target, bending in the vertical plane, can allow us to vary the production angle of the detected particles. A rather large magnet is required (~6 meters

to reach P_T = 3.5 Gev/c). For a number of reasons we prefer the transverse motion method, although the bending magnet method might be attractive in an initial beam survey phase in the proton beam tunnel as discussed in Section 9.

To cover the "backward" region, we use a fixed length spectrometer pivoted around the target. A drawing of the layout is given in Figure 2b. The magnet M_1 is the same as is used in the "forward" configuration, as are the entrance chambers, readout electronics, software, etc. Special chambers, somewhat larger than the ones for the "forward" configuration, are used after the magnet to make up for the loss of aperture arising from the fact that the magnet length is now a significant fraction of the total spectrometer length. A Berkeley-type 13 x 24 C magnet is shown for M_1. At full excitation the momentum band covered is 0.5 to 1.0 Gev/c; lower momenta are obtained by reducing the excitation. The laboratory angle coverage extends from 25 to 155 degrees.

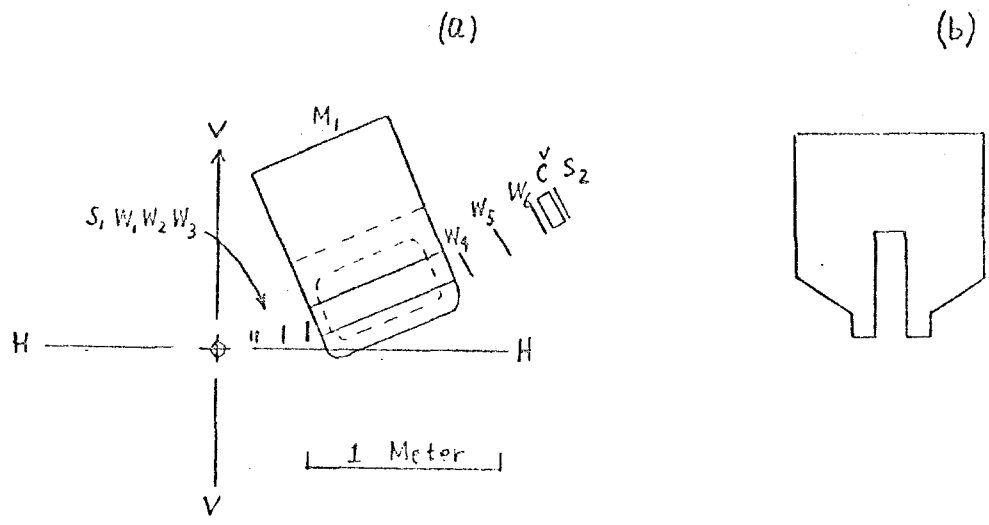

Figure 2b. The low momemtum ("backward") spectrometer configuration: (a) side view; (b) section through magnet. The spectrometer is shown at 90° laboratory angle, with the beam coming out of the paper. HH is the horizontal plane through the target. The entire spectrometer assembly is bolted together and pivots about the vertical axis VV through the target. Laboratory angles of 25 to 155 degrees can be reached.

4. KINEMATICS

In this section we discuss some kinematical features of inelastic scattering at high energies. In particular we exhibit the limiting forms that the relation between laboratory and c.m. quantities take under typical high energy conditions, when the longitudinal momentum of a particle is large compared to its transverse momentum and mass. The experiment is designed to exploit these relationships.

Let the laboratory 4-momenta of particles a, b and c in the reaction $ab \to cd$ to be given by

$$p_a = (E_a, P_a, 0)$$

$$p_b = (M, 0, 0)$$

$$p_c = (E, P_{\parallel}, P_T)$$

where the components given are the total energy, longitudinal momentum and transverse momentum of each particle, and the masses are $m_a = m$, $m_b = M$ and $m_c = \mu$. The corresponding center of mass quantities are

$$p_a^* = (E_a^*, P_a^*, 0)$$

$$p_b^* = (E_b^*, -P_a^*, 0)$$

$$p_c^* = (E^*, P_{\parallel}^*, P_T)$$

Setting

$$s = (p_a + p_b)^2 = m^2 + M^2 + 2ME_a = (E_a^* + E_b^*)^2$$

we have

$$P_a^* = P_a \frac{M}{\sqrt{s}}$$

or, at high energies

$$P_a^* \simeq \sqrt{\frac{MP_a}{2}}$$

For the laboratory longitudinal momentum we have

$$P_{||} = \frac{MP_a}{s} \left[x(E_a + M) + \sqrt{x^2 P_a^2 + \frac{\mu^2 + P_T^2}{M^2} s} \right]$$

where we have introduced the center of mass longitudinal fraction

$$x = \frac{P_{||}^*}{P_a^*}$$

For fixed x, the high energy limit of this is

$$P_{||} \simeq \tfrac{1}{2} \left[xP_a + xM + |x| P_a \sqrt{1 + \frac{x_o^2}{x^2}} \right]$$

where

$$x_o = \frac{\sqrt{\mu^2 + P_T^2}}{P_a^*}$$

The quantity x_o corresponds in size to what Feynman calls "wee" (as opposed to"small") x : wee x means $|x| \leq \frac{1 \text{ Gev/c}}{P_a^*}$, while small x means simply $x \ll 1$.

For positive x we have the following simple limiting relation between $P_{||}$ and x:

$$P_{||} \simeq xP_a, \quad \text{for } x_o \ll x \leq 1$$

In other words, the longitudinal fraction in the lab is the same as the longitudinal fraction in the center of mass, and

is independent of masses.

For negative x we have a different kind of limiting behavior:

$$P_{\parallel} \simeq \frac{M}{2} x - \frac{\mu^2+P_T^2}{2M} \frac{1}{x}, \text{ for } -1 \leq x << -x_o$$

In other words finite $P_{\parallel}$ in the lab corresponds to a definite value of x in the center of mass. The scale factor for the dependence is set by the target mass M and the produced particle mass μ, without any dependence on the incident particle mass m.

The values of $P_{\parallel}$ for positive and negative x join smoothly on to each other in the region $|x| \leq x_o$, passing through the value

$$P_{\parallel} = x_o P_a \sqrt{\frac{MP_a}{2s}} \simeq \tfrac{1}{2} x_o P_a, \text{ for } x = 0$$

The behavior of $P_{\parallel}$ is illustrated in Figure 3, which shows calculated values of laboratory longitudinal momenta for protons, pions and kaons produced by 30 Gev and 200 Gev incident particles on a proton target. The curves shown are for incident protons and for zero transverse momenta, but the same curves, to within plotting errors, hold for incident pions or kaons, and for transverse momenta $\lesssim$ 1 Gev/c.

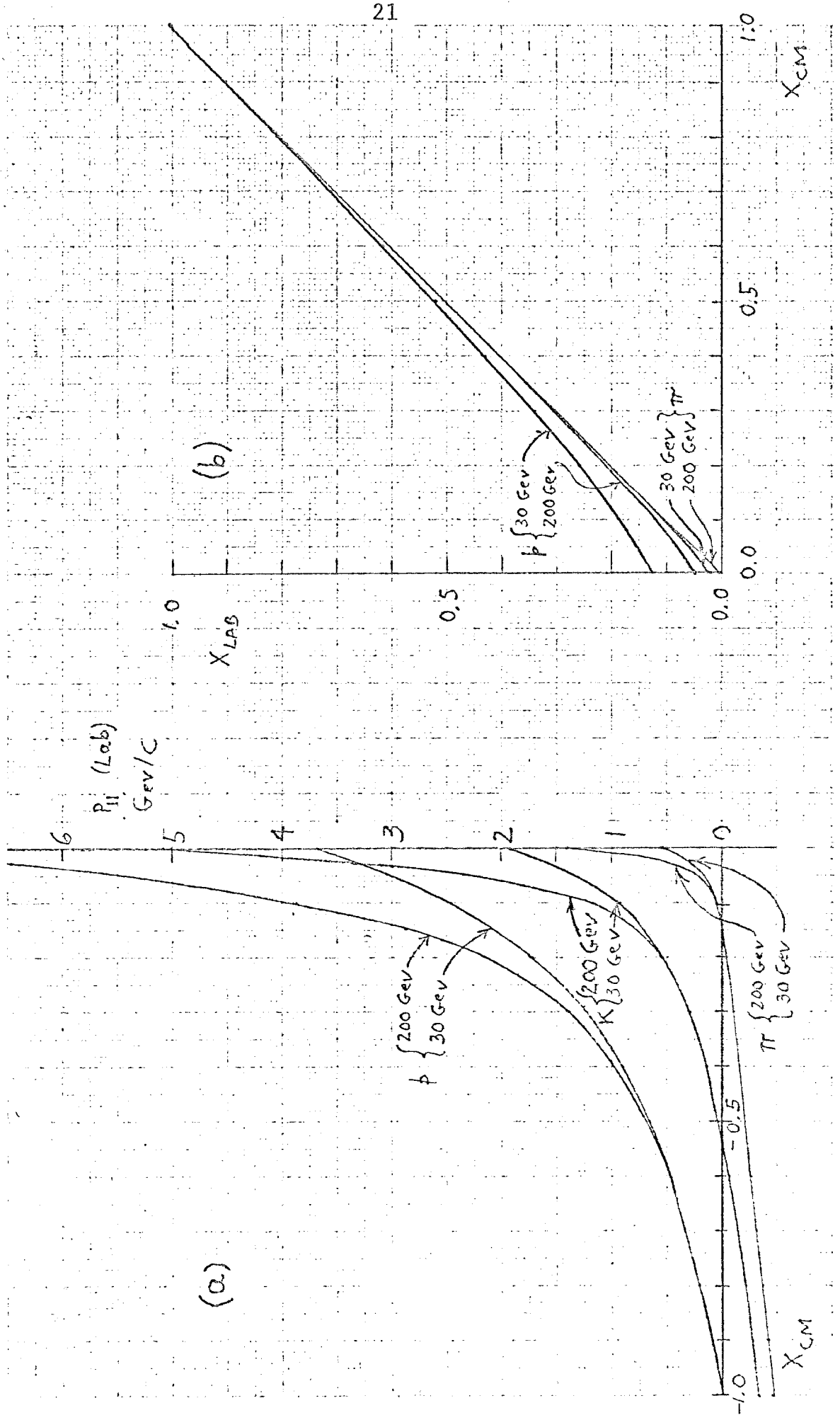

FIGURE 3. Relation between lab and c.m. longitudinal momentum, for zero transverse momentum. (a) The laboratory momentum $P_{\parallel}$ is plotted against x, for $x < 0$, for protons, kaons and pions from pp→p, pp→K and pp→π at 30 and 200 Gev. (b) The quantity $x_{LAB} = P_{\parallel}/P_a$ is plotted against x, for $x > 0$ for protons and pions from pp→p and pp→π at 30 and 200 Gev.

These curves have the following implications for an experimental design. We are interested in covering the entire region of $0 \leq P_T \lesssim 1$ Gev/c and $-1 < x < 1$, including a study of the behavior around $x = 0$. Some information is also useful for larger P_T, over at least part of the range of x. Therefore in the laboratory one should ideally cover the following range of momenta: (a) from the full beam momentum down to ~1 Gev/c at small forward angles corresponding to transverse momenta of $\lesssim 1$ Gev; and (b) from ~1 Gev/c down to zero over the entire range of lab angles from 0 to 180°.

5. SENSITIVITY

We shall parameterize the differential cross section in a simple way suggested by some of the theoretical conjectures in Section 2 to get an estimate of the event rate in terms of the laboratory solid angle and momentum acceptance of our detector. In doing so we are by no means tying the success of our experimental design to the validity of the theoretical conjectures; we are simply using these conjectures as a convenient way to incorporate presently known features of inelastic hadron behavior in the extrapolation to a new energy region. Our experimental design is rather different from what it would be if we had to approach the problem blindly, in which case we would be forced into a considerably more cumbersome and less flexible design.

Without loss of generality we write the differential cross section for $ab \to c$ as

$$\frac{d\sigma}{dx d^2P_T} = \frac{\sigma_o}{\Delta^2} \frac{P_a^*}{E^*} f(P_a^*, x, P_T)$$

where σ_o is the total cross-section for scattering of a on b, $f(P^*_a, x, P_T)$ is a dimensionless function, Δ is a constant with the dimensions of momentum and, as in Section 4, E^* is the c.m. energy of particle c. If limiting fragmentation holds, then f will be a function of x and P_T only, and not of the incident momentum P^*_a. This fact suggests that, in our estimate of the counting rate at high energies, we use the values of f determined in experiments at

existing energies. Furthermore, it appears from data at present energies that f roughly factors into the product of a function of x and a function of P_T. For our estimates it will be convenient to assume that this factorization holds, although this assumption is by no means critical. Thus we are led to the approximate form

$$\frac{d\sigma}{dx d^2P_T} = \sigma_o \frac{P_a^*}{E^*} F(x) \frac{1}{\Delta^2} G(P_T)$$

where $F(x)$ and $G(P_T)$ are dimensionless functions. By definition G is normalized to satisfy

$$\int\int d^2P_T \frac{1}{\Delta^2} G(P_T) = 1$$

From the general nature of the transverse momentum distribution in hadron-hadron scattering we know that, for a value of the constant Δ of the order of 0.4 Gev the function G will be of the order of unity for small P_T, while it will fall off rapidly below unity for P_T large compared to Δ. (An example for which this behavior holds is $\frac{1}{\Delta^2} G(P_T) = \frac{1}{.4^2} e^{-P_T/.16}$).

As for the longitudinal dependence, we have that, for x not "wee",

$$F(x) = \frac{1}{\sigma_o} \int\int d^2P_T \frac{E^*}{P_a^*} \frac{d\sigma}{dx d^2P_T} \simeq \frac{1}{\sigma_o} x \frac{d\sigma}{dx}$$

The data of figure 1 suggest that, depending on the identity of particles a, b and c, $F(x)$ may be of order unity, or it may be smaller

than this by many orders of magnitude, but that it does not exceed a value of the order of unity for x not "wee". As for the "wee" region of x, there are very few data, but the results of Elbert and Erwin[7] for $\pi^- p \to \pi^-$ are consistent with F(x) being well behaved and of order unity for "wee" x.

We have now parameterized the differential cross-section in terms of dimensionless functions F and G which take on maximum values of order unity in some regions of phase space, while falling off to very small values in other regions.

In the remainder of this section we use this parameterization for two purposes: to ensure that the acceptance of our apparatus is not so large that there is a significant probability of two particles from a single event being accepted; and to determine our sensitivity to small cross-sections (values of $F(x)G(P_T)$ small compared to unity). In Section 6 we shall use the parameterization again to ensure that, when our apparatus is set to respond to regions of phase space where the cross-section is small, there is no background contamination from leakthrough of events from regions where the cross-section is large.

First we need to transform our expression for the differential cross-section to laboratory quantities. This transformation is simple; if the laboratory solid angle is $d\Omega$ and the laboratory momentum acceptance is dP, we find

$$\frac{d\sigma}{P^2 d\Omega \frac{dP}{E}} = \frac{\sigma_o}{\Delta^2} F(x) G(P_T)$$

Let

N_i = number of incident particles

N_d = number of detected outgoing particles

F_i = probability that an incident particle interacts

F_d = probability that, given an interaction,
a secondary particle will enter our detector.

Then we have

$$N_d = F_i F_d N_i,$$

$F_i \approx 5\%$ for $\sigma_o = 30$ mb with a 30 cm liquid hydrogen target,

and

$$F_d = F(x)\ G(P_T) \frac{P^2 d\Omega}{\Delta^2} \frac{dP}{E}$$

Thus we see that the quantity $\frac{P^2 d\Omega}{\Delta^2} \frac{dP}{E}$ measures the acceptance of our apparatus, over the entire region of laboratory angles and momenta. Assuming that our apparatus is only able to handle a single particle at a time, we want to make $\frac{P^2 d\Omega}{\Delta^2} \frac{dP}{E}$ small compared to unity in order to ensure that there is only a small probabiltiy of detecting two particles from a single event. The best we can do is to reject any event for which there are two or more particles seen, and apply an appropriate correction to the overall normalization. If there are no correlations we do not thereby make any error, but since in general there may be correlations between

particles in various regions of phase space, we want to be sure that the fraction of events thus rejected is small.

As for the sensitivity to small cross-sections, the apparatus to be described in this proposal will be characterized by an acceptance of

$$\frac{P^2 d\Omega}{\Delta^2} \frac{dP}{E} \approx 1 \times 10^{-2}$$

roughly independent of momentum. We take the lower limit of our experimental sensitivity to be given by a cross-section such that we detect 100 events per hour, or about 0.1 event per pulse at NAL. Assuming a 30 mb. total cross-section and a 30 cm. liquid hydrogen target, we thus have an experimental sensitivity extending down to

$$F(x)\ G(P_T)\Big]_{min} = 2 \times 10^{-6} \times \left[\frac{10^8 \text{ particles/pulse}}{\text{incident Beam Rate}}\right]$$

or, in terms of the minimum detectable laboratory cross-section,

$$\frac{d\sigma}{d\Omega dP}\Big]_{min} = 3.7 \times 10^{-29} \frac{cm^2}{Sr\text{-}Gev/c} \times \frac{10^8 \text{ particles/pulse}}{\text{Incident Beam Rate}} \times \frac{P}{100 Gev/c}$$

It should be remembered that, although pion and proton rates will indeed be 10^8/pulse or higher, the rates of $\bar{p}$'s and K's will be considerably less, and thus we will need all the experimental sensitivity we can get to be able to obtain useful information with these relatively rare particles.

6. BACKGROUNDS AND MAXIMUM BEAM INTENSITY

There will be a maximum beam intensity above which accidental rates will be excessive. The principal limitation is that singles rate in the wire chambers. Using multi-wire proportional chambers with ~100 nsec time resolution, singles rates of $\sim 10^6$ counts/second can be handled. A typical event will then contain the tracks of a true secondary particle within our momentum acceptance, along with accidental counts from particles that registered in a few of the chambers only. Our events are considerably over-constrained, so we can easily reject a few spurious counts. Specifically, we require that the input track form a straight line pointing to the target, the output track from a straight line, and that the two tracks meet properly inside the magnet gap.

The background may be divided into two categories: secondary particles produced in our target, and background not associated with our target.

Using the rate estimate developed in Section 5, we can set an upper limit on the singles rate from secondary particles. Consider a beam of N_i particles per second incident on a 30 cm. liquid hydrogen target, with a small counter of area a^2 located a distance L downstream and $b << L$ transverse to the beam (see Figure 4). The singles rate will then be, according to the model of Section 5,

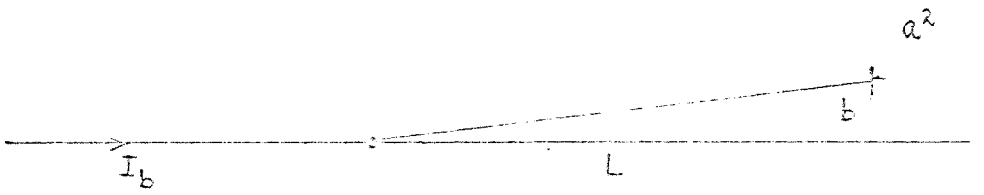

Figure 4. Illustrating the singles rate calculation of Section 6.

$$N_s = F_i F_d N_i$$

where F_i will be ~5%, F_d is given by

$$F_d = \int_0^{P_a} F(x)\ G(P_T)\ \frac{P^2}{\Delta^2}\frac{a^2}{L^2}\frac{dP}{E}$$

and

$$P_T = \frac{b}{L} P$$

To obtain an upper limit on F_d, we replace $F(x)$ by 1, E by P and we extend the upper limit of integration to infinity. Then we find, using the normalization condition on G from Section 5,

$$F_d \leq \int_0^{\infty} G(\frac{b}{L} P)\ \frac{P^2}{\Delta^2}\frac{a^2}{L^2}\frac{dP}{P} = \frac{a^2}{b^2}\int_0^{\infty}\frac{uG(u)\,du}{\Delta^2} = \frac{a^2}{2\pi b^2}$$

This upper limit on the singles rate is independent of the longitudinal distance L, thus encouraging us to use a variable length spectrometer.

Our design is such that, with the apparatus set at the minimum accessible value of P_T,

$$\frac{a^2}{2\pi b^2} = 0.07$$

(see Section 8). Thus we find that target-associated background limits the beam rate to 0.5×10^8 particles per second at the lowest P_T setting.

It is difficult to give a precise estimate of the effects of background from beam halo and general room background. The maximum useable beam intensity will in any case depend on the momentum setting and angle of the spectrometer. On the basis of our experience at lower energy accelerators, we feel that we can safely expect the spectrometer to be able to handle an incident beam intensity of 10^8 particles/second.

7. PARTICLE IDENTIFICATION

We plan to use threshold Čerenkov counters to identify protons and kaons. Such a counter is simply a length of tubing, filled with gas at the appropriate pressure, with a 45^{o} mirror and a phototube at the downstream end. Different lengths will be used depending on the momentum range being studied, as discussed below. Wire chambers before and after the counters will ensure that only one particle has traversed the counter, and will help reject spurious counts arising from interactions with the gas and windows. At the very lowest momenta we may also use dE/dX or time of flight to identify particles. Rejection ratios of 10^{4}:1 should be obtained readily.

Muons and electrons will be identified by means of a shower counter for electrons followed by a thick absorber and a counter for muons. Quark identification is discussed in Section 9.

Threshold Cerenkov counters were built by Gorin et al[10] for use at Serpukhov, using quartz optics. Their measured threshold curves correspond to an average number of photoelectrons of

$$N_e = 1.6 \times 10^{4} \; \eta^{2} L$$

where η is the Cerenkov angle and L is the counter length in meters. Useful signals were obtained from single photoelectrons. We assume that we can equal this performance.

To identify pions at momenta below some maximum value P_{max}, there will be a counter whose threshold for counting K's is at P_{max}. If we demand an average of 10 photoelectrons from pions

of momentum P_{max}, we find that the required length is

$$L = 29 \left(\frac{P_{max}}{100} \right)^2 \quad \text{meters}$$

where P_{max} is in Gev/c. The Cerenkov angle is

$$\theta = 4.7 \times 10^{-3} \left(\frac{100}{P_{max}} \right) \quad \text{radians}$$

and the radius of the Cerenkov cone is

$$a = \theta L = 0.14 \left(\frac{P}{100} \right) \text{ meters.}$$

The counter will cease counting pions entirely at a momentum of $\frac{m_\pi}{m_K} P_{max} = 0.28\ P_{max}$; it will give 7 photoelectrons ($e^{-7} = 0.9 \times 10^{-3}$) at a momentum of

$$P_{min} = 0.51\ P_{max}$$

A second such counter, set at proton threshold, will identify kaons. We find

$$L = 10 \left(\frac{P_{max}}{100} \right)^2$$

$$\theta = 8.0 \times 10^{-3} \left(\frac{100}{P_{max}} \right)$$

$$a = 0.08 \left(\frac{P_{max}}{100} \right)$$

and

$$P_{min} = 0.72\ P_{max}$$

To find the amount of gas required we use

$$n-1 = \frac{m^2}{2\,P_{max}^2}$$

$$= \begin{cases} 1.2 \times 10^{-5} \left(\frac{100}{P_{max}}\right)^2 & \text{for separating k's from } \pi\text{'s} \\ 4.5 \times 10^{-5} \left(\frac{100}{P_{max}}\right)^2 & \text{for separating p's from k's} \end{cases}$$

Since the gas pressure goes as $1/P_{max}^2$ while the counter length goes as P_{max}^2, the number of grams per cm^2 is independent of P_{max}. For example for air or CO_2 we require 0.1 g/cm^2 of Čerenkov radiator for each of the two counters.

8. SYSTEM ACCEPTANCE, RESOLUTION AND OTHER PERFORMANCE FACTORS.

Figure 5 is a simplified view of the spectrometer, with longitudinal and transverse distance parameters L, L', a, and b defined. Let P_o denote the central momentum (the momentum of a particle which goes through the center of each chamber). The solid angle acceptance at P_o is then determined by the aperture of the last chamber, (a square of side a), and has the value

$$d\Omega_o = \frac{a^2}{L^2}$$

The overall scale of the system is determined by the quantity L/P_o, which in our design has the value

$$\frac{L}{P_o} = 1.87 \text{ meters/Gev}$$

Since we vary the spectrometer linearly with momentum, the transverse momentum acceptance $P_o^2\, d\Omega_o$ is independent of P_o.

The solid angle acceptance as a function of momentum is shown in Figure 6. There is a 2:1 range of useful acceptance extending from

$$P_{min} = 0.75\ P_o$$

to

$$P_{max} = 1.5\ P_o.$$

The solid angle averaged over this range is $\overline{d\Omega} = 0.84\ d\Omega_o$, and so the acceptance in invariant phase space is, for a = 0.1 meter,

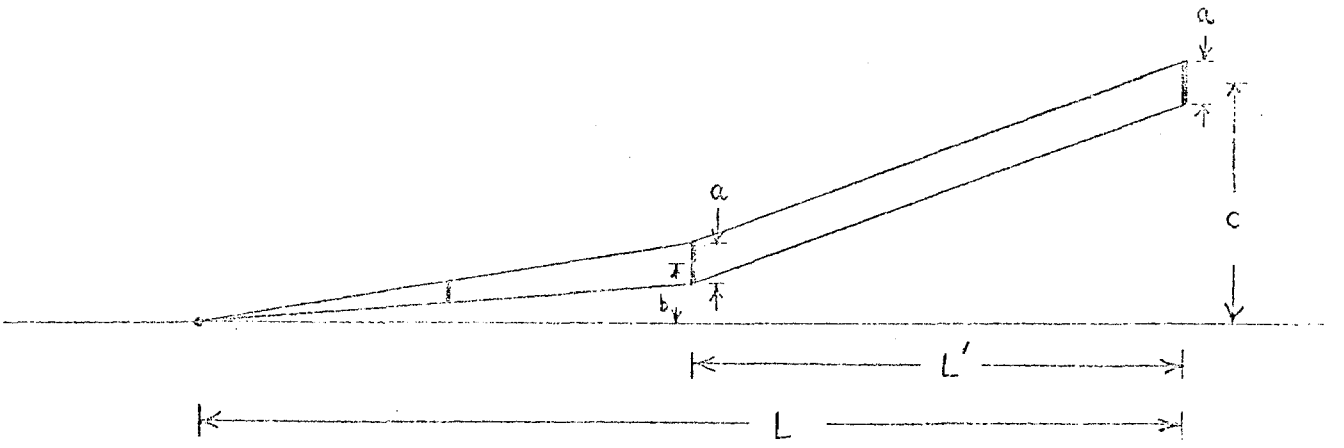

Figure 5. Simplified view of the spectrometer

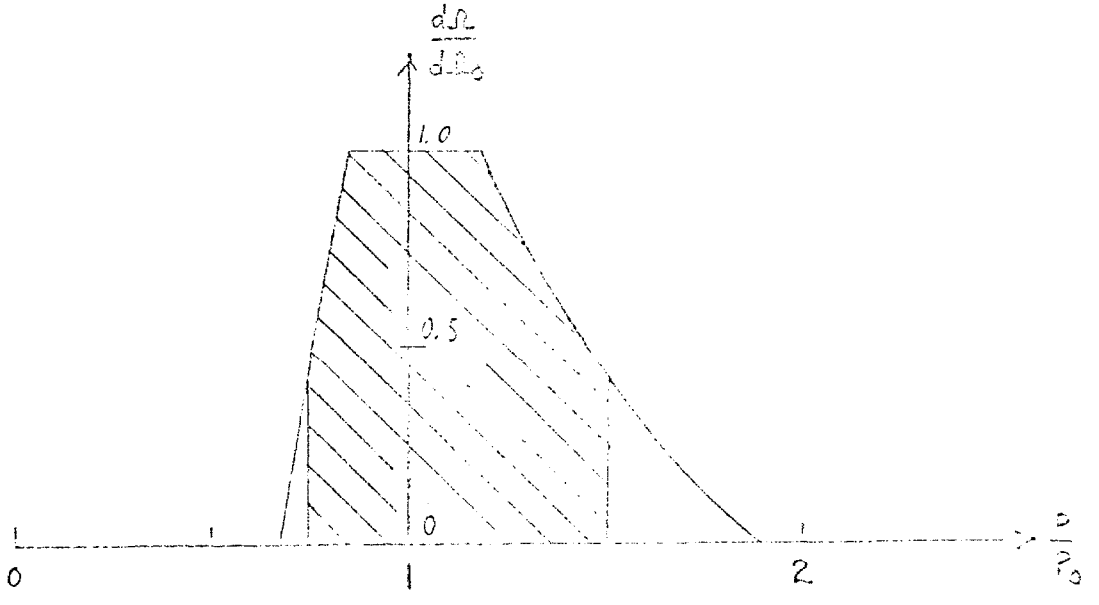

Figure 6. Solid angle versus momentum. The region from P/P_o=0.75 to P/P_o=1.5 is shaded.

$$P^2 \, d\Omega \frac{dP}{E} = P_o^2 \times 0.84 \, \overline{d\Omega} \, \frac{1.5P_o - 0.75P_o}{P_o}$$

$$= 1.8 \times 10^{-3} \ (\text{Gev/c})^2$$

independent of P_o. Expressed in terms of the characteristic transverse momentum Δ = 0.4 Gev/c of Section t, the acceptance is

$$\frac{P^2 d\Omega}{\Delta^2} \frac{dP}{E} = 1.1 \times 10^{-2}$$

The minimum detectable transverse momentum at $p = P_o$ depends on the transverse distance b in Figure 5. For the value b = 0.15 meters it has the value

$$P_{T,min} = 0.13 \text{ Gev/c}$$

The quantity used in Section 6 to put an upper limit on the target-associated singles rate is

$$\frac{a^2}{2\pi b^2} = 0.07$$

The magnet M_1 has a transverse momentum impulse of

$$\Delta P_{mag} = 0.32 \text{ Gev/c} = 0.7 \text{ meters} \times 15 \text{ Kg}$$

The momentum resolution is then determined by two factors: wire chamber resolution and multiple scattering. In a simple worst-case model, we assume that only the information from the

end chambers W_1, W_3, W_4, and W_6 is used, and that the momentum is determined from the difference of the slopes before and after the magnet. Assuming an r.m.s. position resolution of 0.5 mm in each chamber, the momentum resolution due to chamber position resolution is

$$\left.\frac{\delta P}{P}\right]_{\text{chamber}} = 0.5\%,$$

independent of P_o. The momentum resolution due to multiple scattering depends on the quantity ΔP_{scatt}, the r.m.s. transverse momentum from multiple scattering, through the relationship

$$\left.\frac{\delta P}{P}\right]_{\text{scatt}} = \frac{\Delta P_{scatt}}{\Delta P_{mag}}$$

The quantity ΔP_{scatt} is the sum of contributions added in quadrature from multiple scattering in the chambers, Čerenkov counter and vacuum pipe windows, Čerenkov counter gas, and air gaps along the entire path from the first to the last chamber. The scattering contribution from each element is weighted by a factor which varies linearly from unity for components near the magnet to zero for components near W_1 or W_6. We calculate

$$\Delta P_{scatt} = 0.02 \text{ Gev/c}; \quad \left.\frac{\delta P}{P}\right]_{\text{scatt}} = 0.6\%$$

and the overall momentum resolution is

$$\frac{\delta P}{P} = 0.8\%$$

This value is more than adequate for the physics we are studying.

The multiple scattering quoted assumes that we can make plane, 45^{o} mirrors for our Cerenkov counters by depositing a suitable reflective surface on thin foils. We have not yet verified this assumption by actually making such a mirror; however even if a thin glass mirror were required, $\frac{\delta P}{P}$ would be acceptable.

The momentum bite is well matched to the useful momentum range of the pion Cerenkov counters. We will need two kaon Cerenkov counters, set at different pressures, in order to cover the entire momentum range for kaons at once.

The distance L' must be enough to accomodate the Cerenkov counters. This condition can be met up to some maximum momentum. If there is to be enough room to accomodate the pion counter and one kaon counter (the other kaon counter can, at the highest momenta, be put just before the bending magnet or just after the last chamber), we must have

$$(29 + 10)\ (\frac{P_{max}}{100})^2 \leq L' = \frac{1}{2} \times 1.87\ P_o = .62\ P_{max}.$$

Thus

$$P_{max} = 160\ \text{Gev/c}$$

is the highest momentum at which we can have 10^4:1 particle identification over the full momentum acceptance of the

spectrometer. Identification can be accomplished at higher momenta if separation only up to momentum P_o is required:

$$(29 + 10)\ \left(\frac{P_o}{100}\right)^2 \leq L' = \frac{1}{2} \times 1.87\ P_o$$

$$P_o \leq 250\ \text{Gev/c}$$

We can reach 300 Gev/c by relaxing our requirements to 10^3:1 identification.

9. BEAM SURVEY AND QUARK SEARCH

Our principal interest, and the objective around which our apparatus has been designed, is the study of inelastic scattering phenomena with a proton target and a variety of incident particles. Our apparatus can also play a useful role in the intital program of beam surveys and searches for new particles which may be carried on before secondary beams become available.

We believe that it is logical to divide such a program of beam surveys into several complementary experiments. Our apparatus is well adapted to a broad survey of the high-rate, low momentum transfer region. It will quickly provide the engineering information needed for beam design, and it will detect quarks if they are produced $\geq 10^{-4}$ times as copiously as $\bar{p}$'s.

The apparatus will be set up in its 100-200 Gev/c configuration (250 meters overall length), with 200 Gev protons from the external proton beam incident on a nuclear target. Coverage will be obtained down to 25 Gev/c secondary momentum in three momentum bands obtained with full, one half, and one fourth of the design magnetic field. The momentum resolution and acceptance for lower bands will be less than in the variable length design, but will still be more than adequate for a beam survey.

Data will be taken at constant lab angle. Coverage of the desired angular range will be obtained by means of transverse motion of the spectrometer components as discussed in the previous section. The required floor width of the experimental area is of course proportional to the maximum laboratory angle we wish to reach. To obtain coverage out to 15 mrad, we need an area extending out 3.5 meters on one side of the beam center line.

If the needed transverse room is not available, we can keep the spectrometer components fixed over the beam line and use deflecting magnets to vary the transverse momentum, as discussed in Section 3.

The apparatus can easily seek quarks simultaneously with the beam survey. Assuming a minimum detectable quark rate of 1 per hour $\left(\frac{d\sigma}{d\Omega dp}\right)_{lab} \approx 10^{-31}$ cm^2/sterad-Gev/c), rejection ratios of roughly 10^8: 1 against π^-, K^-, $\bar{P}$, and antideuterons will be required.

. Anticoincidence with the Cerenkov counters for identifying π, K and $\bar{p}$ should provide at least 10^4:1 rejection. Two dE/dx counters set to accept particles with ionization rates of .1 to .6 minimum will reject the leakage of π^-, K^- and $\bar{p}$ from the Cerenkov counters, and also any antideuterons, antihelluus etc. Assuming 225 photoelectrons and 10% uniformity of pulse height across the counters, a rejection ratio of 10^4:1 for

each counter is calculated. Because of the Landau tail the efficiency for detecting charge 2/3 quarks will be about 50 per cent. (These counters can also be gated to accept particles of charge 2 or greater, and thus count antihelium. The wire chambers would verify that only one particle was being counted.)

A third dE/dx counter will be pulse height analysed with each event. The resulting spectrum for events satisfying the quark trigger would show peaks with a characteristic Landau distribution from charge 1/3 and 2/3 quarks, as well as any particles leaking through the trigger.

The momentum of any quarks found will be known from their trajectories through the spectrometer. A rough value for the quark mass will be attained by measuring the particle's time of flight through the apparatus. For example, a charge 2/3 quark with 50 Gev/c true momentum will have a time of flight difference of $1.5[M_{quark}/5\ \text{Gev/c}^2]^2$ nsec. Of course, if a tantalizing peak is observed, the precise mass will be determined by a Cerenkov counter pressure curve.

The maximum quark mass observable in the reaction $pp \rightarrow pp q\bar{q}$ at 200 Gev/c beam momentum is

$$M_{quark} = .5\ (\sqrt{s}\ - 2M_p) \approx 8.8\ \text{Gev/c}^2.$$

This mass quark would have a lab momentum of

$$\beta_{cm}\,\gamma_{cm}\,M_{quark} \approx 90 \text{ Gev/c}.$$

For charge 2/3 and 1/3 quarks this corresponds to spectrometer momentum settings of 135 and 270 Gev/c, respectively. Lower mass quarks would have a range of lab momenta. For example, a 5 Gev/c^2 quark could have lab momenta between 16 and 165 Gev/c.

10. RUNNING TIME

A. Beam Survey - 150 hours total

Setup and counter tests-100 hours

Survey and quark search - 50 hours

Laboratory angles of 2.5, 3.5, 7.5 and 15 mr will be covered for secondary momenta of 25-50, 50-100, and 100-200 Gev/c. Crude rate estimates indicate that we will get better than 10% statistics on particle yields for any feasible NAL beam in the momentum range 25-200 Gev/c. The quark search will be combined with the negative particle survey at 2.5 and 3.5 mr for the highest momentum range, and will take 20 hours.

B. Forward Spectrometer-total 450 hours

Testing - 30 hours (in addition to the beam survey setup time).

Changeover checkout and counter efficiency tests-70 hours (7 configurations, and 12 hours for each changeover).

Running time - 350 hrs.

We plan to cover the range of secondary momenta from 1.25 to 160 Gev/c in 7 configurations. For each configuration, beam momenta of 160, 80 and 40 Gev/c will be used (except, of course the high momentum configurations won't be used at lower beam momenta). Cross-sections for six to eight transverse

momenta, and four charge combinations (beam + and -, secondary + and -) will be measured. Individual runs will take from 20 min. to $1\frac{1}{2}$ hours. We expect to keep empty target rates to less than 10% of full target rates using our ability to trace rays through the apparatus. A modest allotment of empty target time is included in the running time estimate.

C. Backward Spectrometer - total 250 hours

Setup - 50 hours

Running time - 200 hours

Measurements will be taken at 8 angles between 25° and 155°, two secondary momentum ranges, 4 charge combinations and 3 beam momenta.

Total time requested - 350 hours.

11. BEAM REQUIREMENTS

In this section we discuss beam requirements for the study of inelastic hadron-hadron scattering assuming that the accelerator operates at 200 Gev/c. Our spectrometer is capable of studying inelastic scattering at secondary momenta up to 500 Gev/c with particle identification up to 250 Gev/c. We are prepared to contribute to the beam survey program and to study inelastic scattering with 500 Gev/c protons if they are available.

We plan to study inelastic scattering at incident momenta of 40,80, and 160 Gev/c. We require an unseparated beam of positive or negative particles with momentum spread $\frac{\Delta p}{p} = \pm .005$. The beam must have a drift space where the divergence is less than $\pm .02$ mrad to accomodate a DISC Cerenkov counter which can distinguish π's and K's at 160 Gev/c.

The permissable beam divergence at the final image is determined by the uncertainty in the transverse momentum of the incident particle. The divergence must therefore be the smallest at the highest beam momentum and most forward spectrometer geometry. If we limit the uncertainty in transverse momentum under these conditions to $\pm$ 50 Mev/c we obtain a divergence less than or equal to $\pm$ 0.25 mrad. This divergence can be achieved by turning off the focusing magnets between the DISC counter and the hydrogen target and using a large (several centimeter) diameter target. At lower beam momentum or lower secondary laboratory

momentum the divergence at the final image can be larger. When the backward spectrometer is used the hydrogen target should be smaller in diameter (one centimeter) in order that the lowest momentum secondaries see the least possible material in getting out of the target.

The maximum intensity of the beam is limited by the background, and by the maximum rate at which beam particles can be identified. As discussed in Sec. 6, the experiment can use a beam of 10^8 particles/pulse or more.

A beam similar to the 2.5 mrad beam described by Reeder and MacLachlan in the 1969 NAL Summer Study is adequate for our experiment.

For the beam survey, the properties of the incident proton beam must be consistent with the above requirements. In particular, we must be able to reduce the incident proton intensity to 10^8 or 10^9 protons/pulse.

12. EQUIPMENT REQUIREMENTS AND MANPOWER

1) Experimental Area: The experimental area should be 4 to 5 meters wide to one side of the incident beam and 200 meters long. It should include a portable house or trailer furnished by NAL for housing electronics.

2) Liquid Hydrogen Target: We will require a liquid hydrogen target with appendices of two different diameters for the various beam divergences and magnifications used. There must be two appendices of each size of which one is filled with hydrogen and one is empty for target empty runs. We must be able to switch targets by remote control. The targets should be provided by NAL.

3) Spectrometer Magnet: The spectrometer magnet is a C-magnet of a type presently in use at the Lawrence Radiation Laboratory. We expect NAL to borrow an existing magnet or construct a similar one.

4) Spectrometer Mounting and Alignment System: Although this system is simple in principle, it will require a larger engineering effort than we can mount ourselves. For the "forward" spectrometer the motion and alignment of the magnet and detectors transverse to the beam must be accomplished by remote control. Motion parallel to the beam should also be accomplished easily, but will be performed the minimum number of times because a change in

length of the Cerenkov counters is made at these times.

The "backward" spectrometer is simpler in that it pivots about the hydrogen target. It is desirable to control the motion of the backward spectrometer remotely.

We request that NAL provide the spectrometer mounting and alignment system.

5) DISC Cerenkov Counter: The DISC Cerenkov counter for the beam will be provided by the experimenters.

6) Computer Facilities: We require a small computer for data collection and monitoring. We are prepared to furnish this computer ourselves. We will also require fast turn-around (a few hours) access to a large computer for data processing.

In addition to the three authors of this proposal we will have one additional Ph. D. physicist (a research associate), one student, and one technician.

BIBLIOGRAPHY

1. R.P. Feynman, in the Proceedings of the Third International Conference on High Energy Collisions at Stony Brook, and Phys. Rev. Letters 23, 1415, (1969).

2. E. Fermi, Progress of Theoretical Physics 5, 570 (1950).

3. J. Benecke, T.T. Chou, C.N. Yang, and E. Yen, Phys. Rev. 188, 2159 (1969).

4. See also the talks by J.D. Bjorken and S. Drell, Proceedings of the International Conference on Expectations for Particle Reactions at the New Accelerators, April 1970.

5. See F. Gilman, Proceedings of the 4th International Symposium on Electron and Photon Interactions at High Energy, Daresbury Nuclear Physics Laboratory, Daresbury nr. Warrington, England (1969), Ed. D. Braben, and references therein.

6. Diddens et al, Nuovo Cimento 31, 961 (1964); Dekkers et al, Phys. Rev. 137, B962 (1965); Anderson et al, Phys Rev. Letters 19, 198 (1967); Ratner et al, Phys. Rev. 166, 1353 (1968); Allaby et al, CERN PS/6517/kl (submitted to the 14th Conference on High Energy Physics, Vienna, 1968); Day et al, Phys. Rev. Letters 23, 1055 (1969).

7. A.R. Erwin, Proceedings of the International Conference on Expectations for Particle Reactions at the New Accelerators, April 1970.

8. R. Hagedorn and J. Ranft, Suppl. Nuovo Cimento 6, 169 (1968)

9. D. Amati, A. Stanghellini and S. Fubini, Nuovo Cimento XXVI, 896 (1962); G. F. Chew and A. . Pignotti, Phys. Rev. 176, 2112 (1968); S. Pinsky and W. I. Weisberger (unpublished).

10. Yu P. Gorin, S. P. Denisov, S. V. Donskov, A. F. Juanaitsev, A. I. Petrukhin, Yu. P. Prokoshkin, D. A. Stoyanova and R. S. Shuvalov, IHEP Preprint 69-63 (English translation Scientific Translation Service, Order No. 8624, Ann Arbor, Michigan).

ADDENDUM TO N.A.L. PROPOSAL 52

Eugene W. Beier, David L. Kreinick, Howard Weisberg

University of Pennsylvania

November 16, 1970

We have proposed an experiment to measure the differential cross-section for single particle production in the collisions of charged particles with protons. Specifically we proposed to measure $\frac{d\sigma}{d^3p_c}$ for the reaction a + p → c+ anything, where a, c = $p^{\pm}$, $K^{\pm}$ and $\pi^{\pm}$, over the complete range of secondary momenta. The theoretical considerations which motivated our proposal strongly suggest that there is great interest in covering the widest possible range of secondary momenta.

It was suggested by Dr. Wilson that we consider the use of the single-arm spectrometer facility, or the forward arm from the double-arm spectrometers of experiments 7 and 61, to carry out our measurements. As discussed further below, these spectrometers are essentially high-momentum devices, and will be mainly limited to studying particles moving with large positive momentum in the c.m. ($x > 0$, or "Fragments of the Projectile" in Yang's language of Limiting Fragmentation). We wish to emphasize here the importance, among early measurements from N.A.L., of measuring the momentum spectra of particles having relatively small laboratory momenta (and correspondingly large angles). Specifically we refer to particles having momenta near zero in the c.m. (the "wee" momenta which according to Feynman play a fundamental role in hadron-hadron scattering, and particles of negative x ("Fragments of the Target").

It is to be emphasized that there is separate physical interest in measurements in each of the kinematic regions, and that measurements taken in different regions will complement each other. We believe that early measurements from N.A.L. should not be limited to the high-momentum small angle region only.

We suggest that the kinematic region be covered in three phases:

I. Particles going forward in the lab with $1.5 \leq p_{lab} \lesssim 20$ Gev/c.

II. Low momentum, large angle particles ($p_{lab} \lesssim 1.5$ Gev/c).

III. High momentum particles ($p_{lab} \geqslant 20$ Gev/c).

The unique feature of our experiment is its ability to achieve comprehensive coverage of regions I and II. Region III could be covered either by the longer configurations of our proposed apparatus or by apparatus already under construction (for experiments 7 and 61) or by the proposed single-arm spectrometer facility.

We therefore propose that we be authorized to measure at an early date particle spectra in regions I and II. These measurements would be carried out with the short, low-momentum configurations of the apparatus described in our proposal. These configurations are modest in scale and use well-tested detection techniques. Thus we wish to separate the part of our proposal dealing with relatively low laboratory momenta, and we wish to carry out this part first.

In the remainder of this addendum, we discuss our detailed proposals for regions I and II, and various possibilities for region III.

I. Forward particles, $1.5 \leq p_{lab} \leq 20$ Gev/c

This region will be covered by our forward spectrometer as originally proposed, but only in those configurations permitting coverage up to secondary particle laboratory momenta of 20 Gev/c. The total length of the longest (20 Gev/c) configuration is 25 meters. There will be some

coverage up to 40 Gev/c, at reduced momentum resolution, in order to provide overlap with higher momentum data. Fig. 1 is a drawing of the spectrometer in its shortest configuration. The coverage in terms of Feynman's variable x brackets the x=0 region. Depending on transverse momentum, and on the mass of particle c, the coverage in x extends from a lower limit of from x = -0.6 to x = -0.02, continuously up to an upper limit of from x = 0.1 to x = 0.5. In accordance with our original method of estimating running time, the beam time which we are requesting for this phase is 370 hours (including testing).

II. Backward particles of $p_{lab} \lesssim 1.5$ Gev/c

This range will be covered with our backward spectrometer, as originally proposed. Fig. 2 is drawing of the spectrometer. This spectrometer extends the coverage obtained with the forward spectrometer to x = -1.0.

In discussions with the N.A.L. staff, we have determined that there is a real possibility that this phase of the experiment could run in a parasitic mode, upstream of another experiment. Fig. 3 depicts how this can be accomplished, by installing the backward spectrometer in the mezzanine of the Meson Area building. Crane coverage is not required. The target is 10 cm of liquid hydrogen (volume ~ 0.1 liter). The beam requirements could be met by the 2.5 mrad or 3.05 mrad beams, with momenta near 40, 80 and 160 Gev/c and spot size at our target of a few cm. The beam emerges from our experiment undeflected and undisturbed, except for negligible amount of energy loss and multiple scattering. Background produced by our target will be no more than that from counters or other monitors placed in the beam. Of course we are aware of the difficulties, both psychological and logistical, of running experiments in tandem this

way; however, in view of the possibility of increasing the physics output of N.A.L. at little additional investment, we feel that tandem running in this case is worth a try.

The running time needed for the backward phase is 250 hours. Because of the possibility of tandem running, this phase could be carried out at a very early stage of the N.A.L. research program.

III. High momentum particles ($p_{lab} \geq 20$ Gev/c).

A. High-Momentum Configurations of our Original Proposal.

This approach involves an apparatus that is relatively modest in cost, and that is tailored to this specific experiment. Details are given in our proposal.

B. The Strong Focussing Spectrometer Facility.

The device which was discussed at the Single-Arm Spectrometer Workshop would be well suited for studying particle production spectra at large laboratory momenta and small angles.

It was agreed at the workshop that the lower limit of the design range of the spectrometer will be $p_{min} = 20 - 40$ Gev/c. The magnets of course can be tuned lower, but several factors set a useful lower limit for the spectrometer. These are: the maximum accessible scattering. angle of ~80 mrad; the problem of decay of mesons over the long path thru the spectrometer; the small acceptance (in d^2p_T) at low momenta.

We had a discussion with Dr. J. Friedman of M.I.T. who is the chairman of the subcommittee that will prepare the proposal for use of the facility in inelastic scattering. It was agreed that our group would not participate in the activities of this subcommittee but that we would keep in touch and, should both efforts be approved, we would try to coordinate the choice of kinematic regions covered and arrange

for suitable overlap.

C. The Equipment of Experiments 7 and 61.

It seems quite possible that the forward arm of one of these experiments could be used, essentially unmodified, to obtain single particle distributions at high momenta such as 50, 100 and 150 Gev/c. We have not studied this possibility in detail; in particular we are not sure how one would handle the problem of multiparticle contamination (see below). As far as we know, no one is now actively developing the idea of using the forward arm unchanged.

The remainder of this addendum to our proposal is devoted to a discussion of the multiparticle contamination problem, and to some comments on various features of our experiment.

The Multiparticle Contamination Problem.

Multiparticle contamination (see pages 26-27 of our proposal) can be a crucial source of systematic error in a measurement of single particle distributions; it appears that the subtleties of this problem are not universally understood. Imagine a single-arm spectrometer with a Čerenkov counter for particle identification. If the acceptance of the spectrometer is too large, then there will be a significant probability that two particles from a multiparticle event will traverse the Čerenkov counter. (Actually depending on the design, there may be many more particles traversing the counter than are ultimately accepted by the system). Now of course, if there are suitable wire chambers in the spectrometer, one can sort out the trajectories of the two particles. One will then know that two particles were produced in the region of phase space being studied, and one will even know the momentum and angle of each. The problem is that one will now have a class of events without particle identification. Since two-particle correlations may be significant, there

will thus be a unavoidable systematic error in one's results for the single-particle distributions.

Comments On Our Experimental Design.

Our experiment will have the following key features:

1. Direct control over the multiparticle contamination problem.

2. Constant acceptance in d^2p_T, as large as possible consistent with (1). The solid angle in the lab will vary from 5 msr at 1 Gev/c to 50 μsr at 20 Gev/c.

3. Adequate momentum resolution over the entire range of laboratory momenta covered.

Accuracy. In the most favorable parts of the range of the distributions to be covered, the internal accuracy of the experimental normalization will be a few percent. This capability for high accuracy will be particularly important for studying the dependence of the distributions on incoming energy, and the extent to which they approach high energy limits.

Particle Identification. We believe that data for incident and outgoing K's and $\bar{p}$s can be obtained simultaneously with the data for π's and p's, at little incremental effort, because of the way in which our apparatus is designed. In particular we do not think that the extra degree of comprehensiveness will in any way degrade the quality of the data for incident and outgoing π's and p's. Should the situation turn out to be otherwise, we shall of course concentrate on the π and p part of the experiment only.

Spectrometer Motion and Alignment System.

The backward spectrometer is pivoted about the target in a standard way (refer to Fig. 2).

In the case of the forward configurations, we have chosen the unorthodox technique of transverse motion of individual components. We have found that one reasonable way to achieve the motion is by means of precision slides. These slides, along with their driving motors and digital electronics, are stock industrial items made for numerical machine control applications. The position accuracy is typically a factor of ten better than we require. The cost is low. Although the techniques of precision mechanical motion are perhaps unfamiliar to some high-energy physicists, we consider this part of our experimental design to be a simple, dependable and elegant solution to a number of experimental problems. (We are still optimizing the motion system, but are confident that we have already achieved a workable solution). The longitudinal motion provided by rails is to be of coarse accuracy only. If suitable crane coverage is available, we need not use rails at all.

FIGURES

Figure 1.

Plan view of the forward spectrometer in its lowest momentum (1.25-2.5 Gev/c) configuration. Secondary particles from the liquid hydrogen target pass through scintillator S_1, wire chambers W_1, W_2 and W_3, magnet M_1 (Pole tip region shown shaded), chambers W_4, W_5, W_6, scintillation counter S_2, Cerenkov counters C_1, C_2 and C_3, and chamber W_7. A 12C24 (P.P.A. or A.G.S.) Magnet is assumed for M_1. Chambers W_3 and W_4 are located at the edges of the M_1 effective field region, between the M_1 coils. All components are mounted on precision slides to permit motion transverse to the beam under remote computer control. The slides for W_3 and W_4 are mounted directly on magnet M_1 to permit transverse motion relative to it; this extra motion is necessary in the lowest momentum configurations where the M_1 field length is an appreciable fraction of the total spectrometer length. The other five slides are mounted on five trolleys which ride on rails, providing longitudinal motion of coarse accuracy. After each configuration change (there are four forward configurations) the precision slides are leveled and aligned with respect to each other and the beam by means of adjusting screws and jacks (not shown) using standard optical surveying techniques.

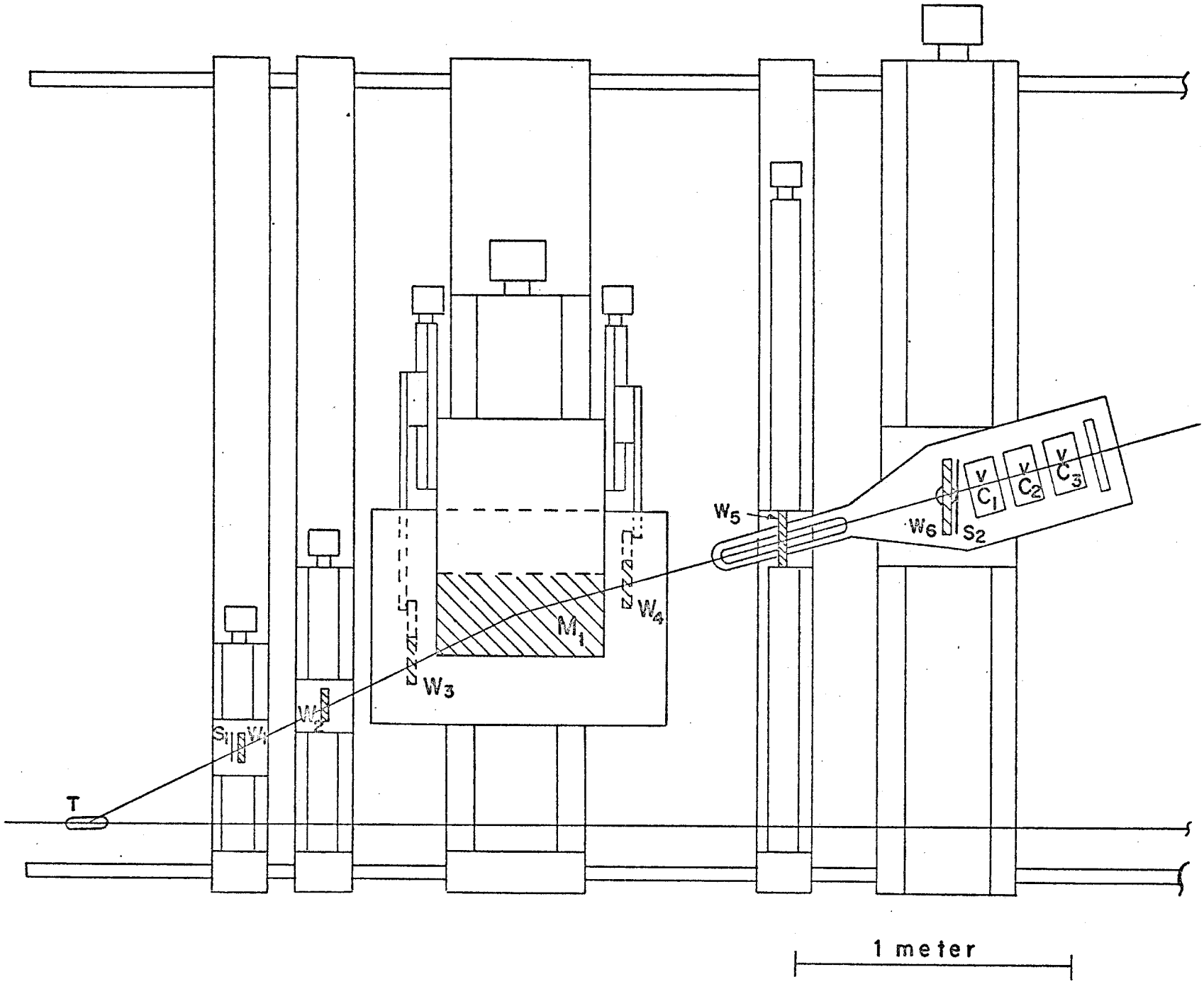
T
S1
W1
W2
W3
M1
W4
W5
W6
S2
V
C1
V
C2
V
C3
1 meter

Figure 2.

Plan view of the backward spectrometer configuration. Secondary particles from the liquid hydrogen target T pass through scintillator S_1, wire chambers W_1, W_2, and W_3, magnet M_1, chambers W_4, W_5 and W_6, scintillation counter S_2, threshold Cerenkov counters C_1, C_2 and C_3, and chamber W_7. A 12C24 (P.P.A. or A.G.S.) magnet is assumed for M_1. The layout differs somewhat from that shown in our original proposal in that both the bending plane and the scattering plane are now horizontal, permitting coverage of a wider range of production angles. Chambers W_3 and W_4 are located at the edges of the M_1 effective field region, between the M_1 coils. All components are mounted on a table, which pivots about an axis through the target, and which rides on a circular rail. The production angle viewed by the spectrometer can be changed and read remotely, under computer control.

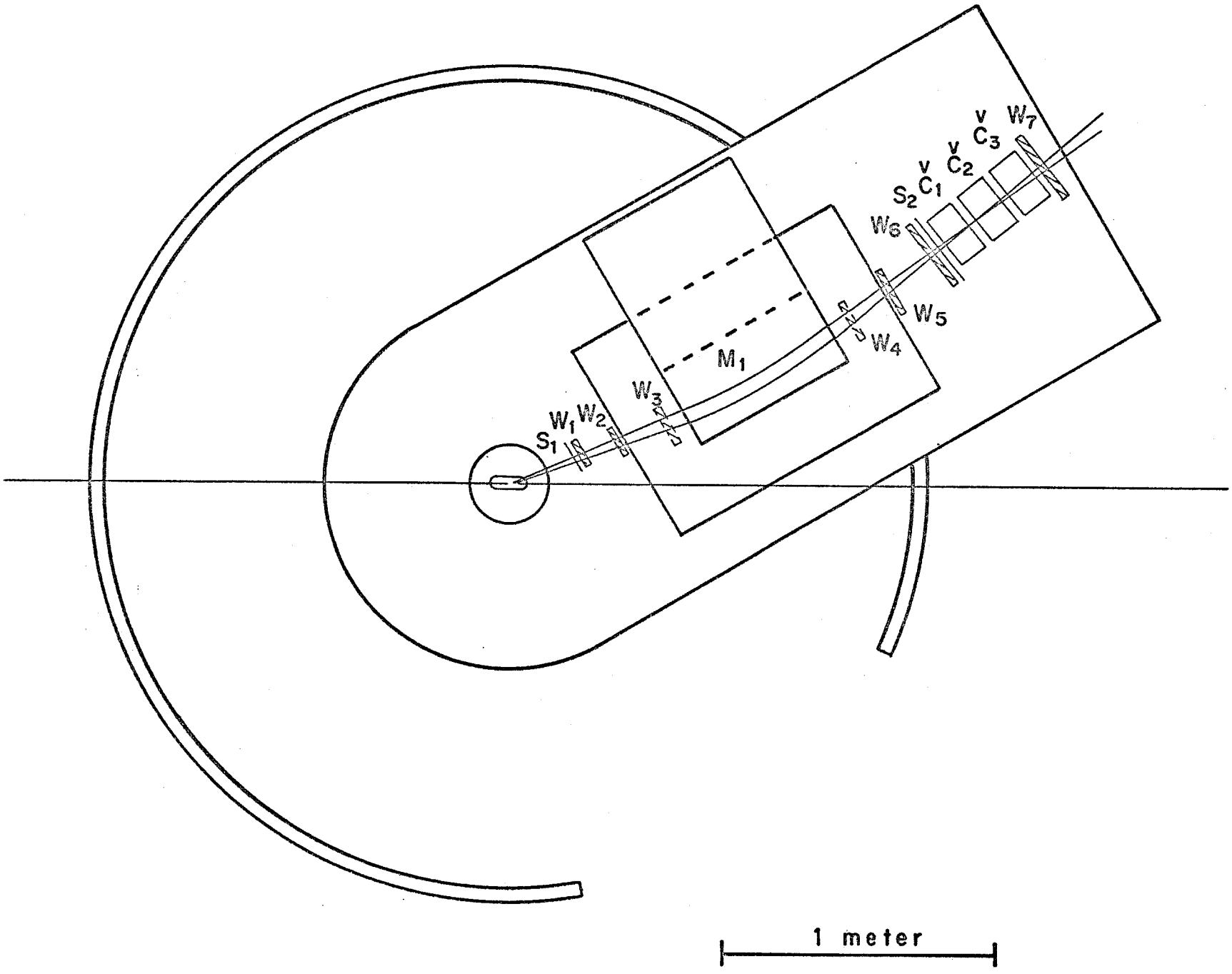
W7
C3
C2
C1
S2
W6
W5
W4
M1
W3
W2
W1
S1
1 meter

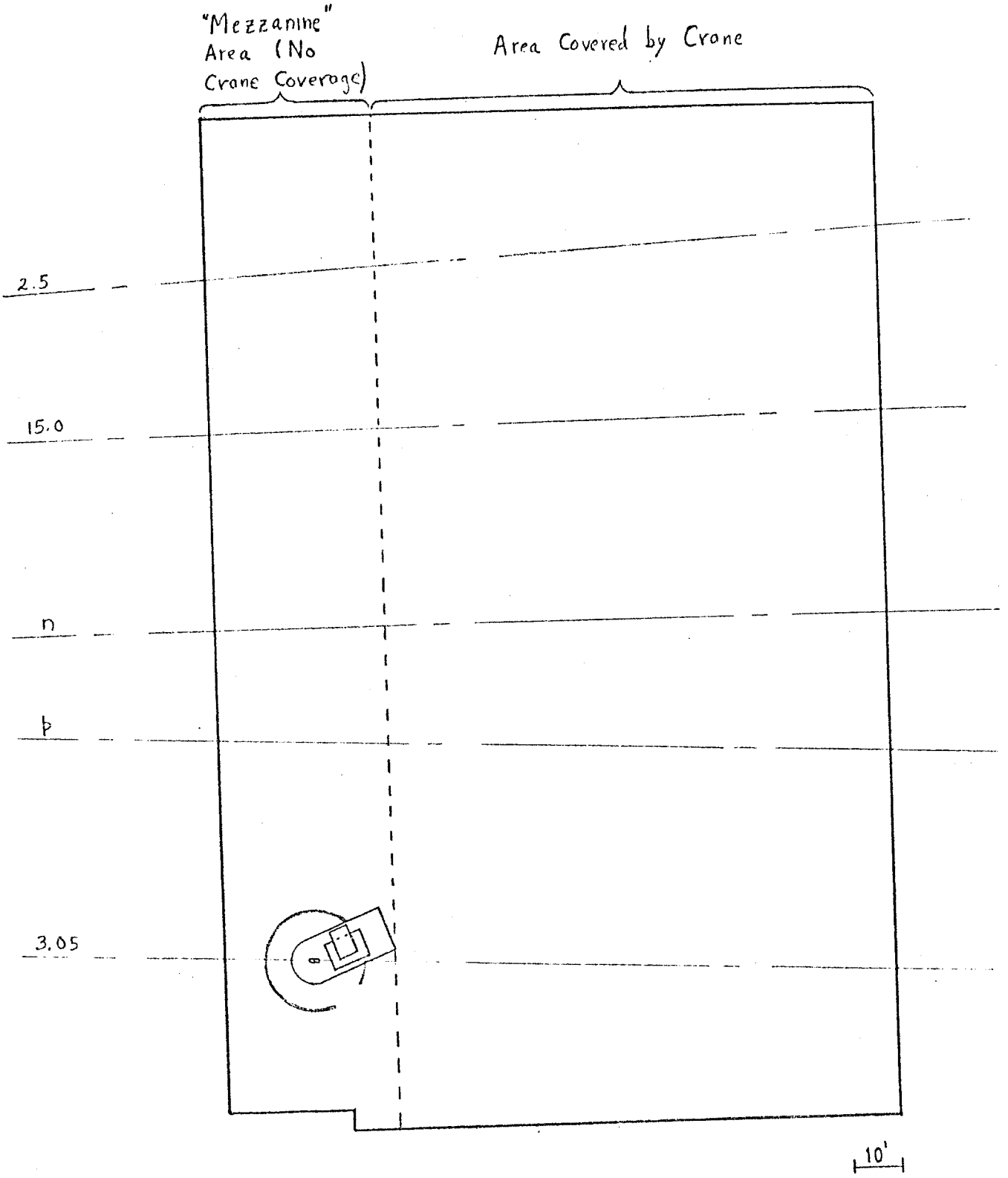

Figure 3.

Plan view of the backward spectrometer installed in the 3.05 mrad beam in the Meson Area, upstream of another experiment. The 2.5 mrad beam will also be suitable.

N.A.L. PROPOSAL 52, ADDENDUM 2

Eugene W. Beier, David L. Kreinick,
Richard Van Berg and Howard Weisberg

University of Pennsylvania

July 19, 1971

Summary - We propose to make a comprehensive set of measurements of "inclusive scattering" for secondary laboratory momenta up to 20 Gev/c, corresponding to the "target fragmentation" region and the "central" region of secondary momenta. The spectrometer we shall use for these measurements consists of a small C-magnet, Charpak chambers, and threshold Cerenkov counters, on a rigid arm that pivots around a vertical axis thru the target. Our experiment can fit into the "front-porch" area in the 3.5 mrad beam upstream of the Meson Building. The spectrometer is the same one we are constructing for our A.G.S. inclusive scattering experiment which will be run during 1972. The demand on N.A.L. resources will be small.

Introduction - We have proposed an experiment to measure the differential cross-section for single particle production in the collisions of charged hadrons with protons. Specifically we proposed to measure $\frac{d\sigma}{d^3P_c}$ for the reactions a + p → c + anything, where a,c = $\pi^{\pm}$, $K^{\pm}$, and $p^{\pm}$, over the complete range of secondary momenta. In an addendum dated November 16, 1970 we described how the range of secondary momenta can be divided into various regions.

In the present (and hopefully last!) addendum, we propose specifically to carry out measurements in the region of secondary momenta $P_{lab} \leq 20$ Gev/c, corresponding to the "target fragmentation" and "central" region of the kinematic range.

This addendum incorporates some small but important design improvements coming out of work we have done this spring and summer on the design of the single-arm spectrometer for our A.G.S. experiment on particle production spectra.

Experimental Layout - Figure 1 is a plan view of our A.G.S. layout, which is identical to our proposed N.A.L. layout. There is a ten-foot arm that pivots around the target from 0 to 270 degrees, and an extension to 30 feet that pivots from 0 to 30 degrees. We have found that, by using the "decision making" capability of Charpak chambers, we can cover a wide momentum range with a fixed-length non-focusing spectrometer. The ten-foot length covers the momentum range from 0.3 to 5 Gev/c in four momentum bands, and the 30-foot length covers 2.5 to 20 Gev/c in three bands, with some capability also up to 40 Gev/c.

Essentially all of the equipment has been designed and is under

construction or prototype testing, except that the arm extension and tracks for the 30-foot configuration have been designed but are not under construction.

The 30-foot configuration uses the same spectrometer drive, angle readout, magnet, wire chambers, cables and electronics as the 10 foot one, and uses some of the same Cerenkov counters. We plan to make the configuration changeover once during the course of the experiment.

We believe the experiment can fit naturally in the "front-porch" area (total length 40 ft.) in the 3.5 mrad beam upstream of the Meson Lab. Alternatively, it could go somewhere else in the 2.5 or 3.5 mrad beams.

Performance Parameters - The properties of the two configurations of our spectrometer are given in Table I. These properties are quite similar to those given in our initial proposal, despite the economies of design which have been achieved.

It is of interest to compare these properties with those of a focusing spectrometer, and so the third column shows the properties of the low-momentum focusing spectrometer being built at N.A.L. for use in the proton beam. In the range up to 2.5 Gev/c, the product (solid angle acceptance) x (momentum acceptance) x (target length) is three orders of magnitude greater for our spectrometer. Therefore, for use in secondary beams, the focusing spectrometer is inadequate.

Experimental Coverage and Time Estimate - Figures 2 and 3 are Peyrou plots showing the coverage of our experiment for secondary pions and protons. Each numbered region shown corresponds to a single "sweep" (sequence of

short runs covering fixed secondary momenta and a sequence of angles.)

Each sweep will be carried out 12 times (3 beam momenta x 2 primary particle charges x 2 secondary particle charges); some additional running with target empty and some repeats of old settings will also be needed. Table 2 gives, for each sweep, the laboratory momenta and angles covered.

In accordance with the original method of estimating running time given in our proposal, the beam time which we request is a total of 750 hours (including testing).

Beam Requirements -

1. Momenta: 40, 80 and 160 Gev/c.
2. Polarities: Both.
3. Momentum Bite: ± 1.0%
4. Angular divergence: ± 2.5 mrad or better
5. Spot size: 1 cm or smaller full width in both planes
6. Halo: Better than 99% of the hadronic component of the beam should be contained within a 4 cm diameter circle.
7. Intensity and disposition of the beam downstream of our experiment: Most of our running will be with the maximum available intensity that the Cerenkov counters can handle, and the beam will pass undisturbed thru our apparatus. Our small angle running requires reduced intensity, and the beam may be deflected ± 2.5 mrad by our spectrometer magnet.

Equipment Requirements -

1. Experimental area: Layout is shown in Figure 1. An enclosed area for housing the electronics should be provided by N.A.L.

2. Liquid hydrogen target: Standard target with 8 inch long, 2 inch diameter flask. We no longer require remote changing from full to empty target.

3. Spectrometer magnet: One 12C24 magnet. Its power supply should have low ripple to prevent vibrations in the Charpak chambers which are placed in the magnet fringe field.

4. Spectrometer mounting and alignment system: To be furnished entirely by us. If there is no crane coverage, then a fork-lift truck is needed for initial installation of the tracks and magnet, and once during the experiment to move the magnet for the configuration changeover.

5. Beam instrumentation: To be provided by N.A.L. for simultaneous identification of pions, kaons and protons.

6. Computer facilities: We no longer are assured that the University of Pennsylvania PDP-9 computer, which we shall be using at the A.G.S., will be available for N.A.L. use. Therefore we request that N.A.L. provide a PDP-15, PDP-11 or similar computer with at least 8K of memory, a high-speed tape drive, a CRT display, and a CAMAC interface.

We also require either an on-line link or else fast turn-around (a few hours) off-line access to a large floating-point computer.

Manpower - The experiment will be manned by physicists from the University of Pennsylvania.

Schedule - Our A.G.S. experiment is scheduled to go on the floor in February 1972, and to be finished by the end of 1972. This schedule has not slipped at all since last December and we expect that it will be met. Therefore, we propose being installed at N.A.L. in January, 1973.

TABLE 1

SPECTROMETER CHARACTERISTICS

	This Proposal		N.A.L.-Walker*
	Short Configuration	Long Configuration	
Type	Non-Focusing, Rotatable	Non-Focusing, Rotatable	Focusing, Rotatable
Length, ft.	10	30	24
P_{max}, Gev/c	5	20	2-2.5
θ_{min}, degrees	6-12**	2-4**	5
θ_{max}, degrees	180	30	175
$\Delta P/P_{central}$	75%	75%	10%
δ_p, %	0.4-1.0 r.m.s.	0.4-0.8 r.m.s.	±1.2
L_{target}, cm	10	10	1
$\Delta\Omega$, sr	5×10^{-3}	0.5×10^{-3}	0.2×10^{-3}

* Figures given by J. K. Walker at 1971 N.A.L. Users' Meeting.

** Limited by multiparticle contamination.

TABLE 2

KINEMATIC REGIONS COVERED*

Sweep	Configuration	Lab Momenta, Gev/c	Lab Angles, Degrees
I	10 foot	0.31 - 0.63	6 - 180
II	"	0.63 - 1.25	6 - 120
III	"	1.25 - 2.5	9 - 75
IV	"	2.5 - 5	12 - 50
V	30 foot	2.5 - 5	2 - 12
VI	"	5 - 10	3 - 30
VII	"	10 - 20	4 - 15
VIII	"	20 - 40	**

* The actual range of momenta and angles covered in each sweep will be somewhat larger than shown, to allow for overlap.

** Some running can be done at 20-40 Gev/c to provide overlap with other experiments.

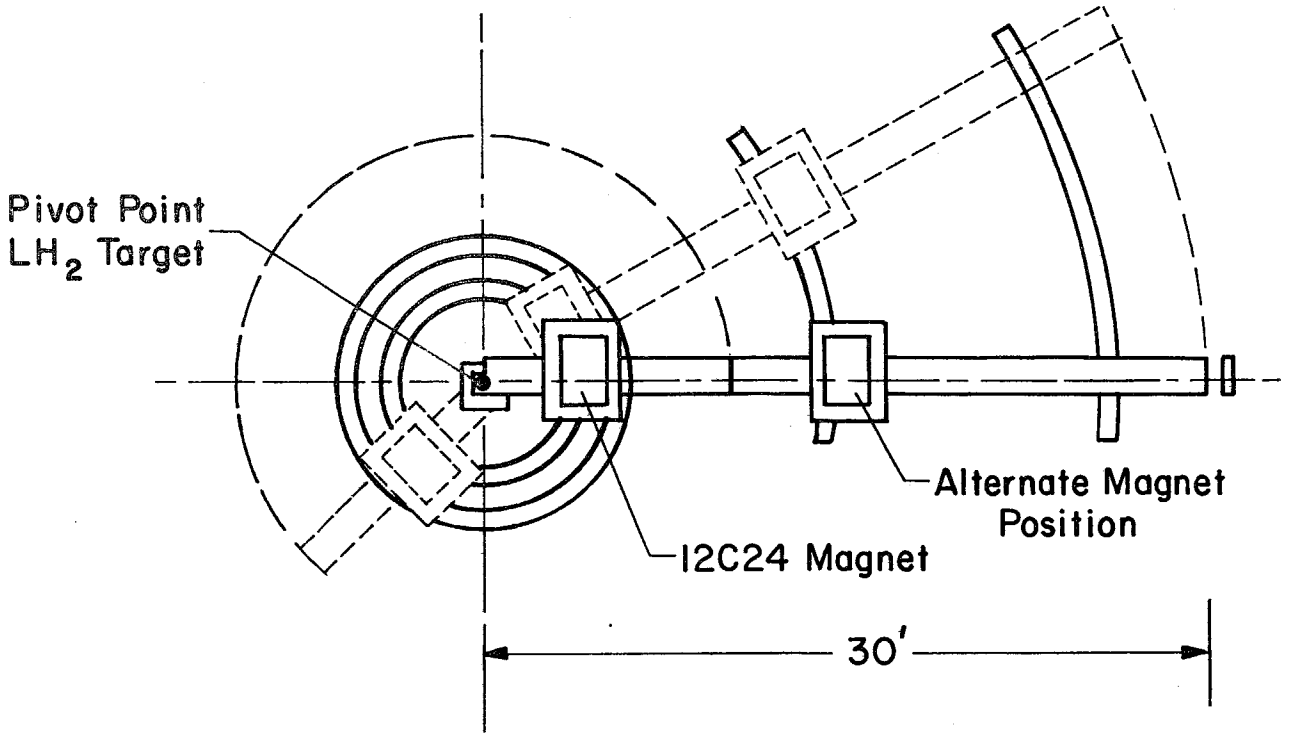

Figure 1. Overall layout of the experiment.

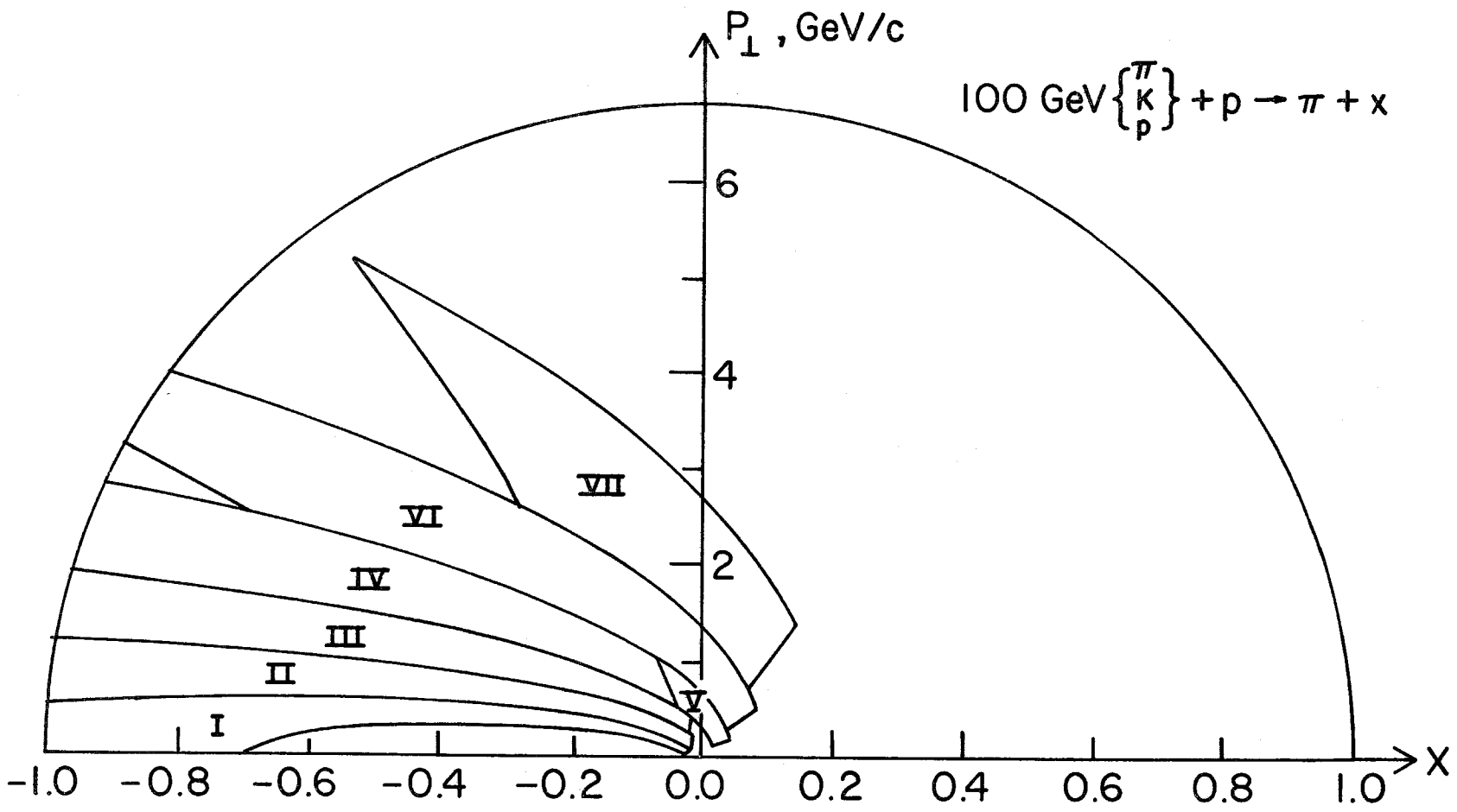

Figure 2. Peyrou plot showing the kinematic region covered in our experiment for the production of pions by 100 Gev pions, kaons or protons.

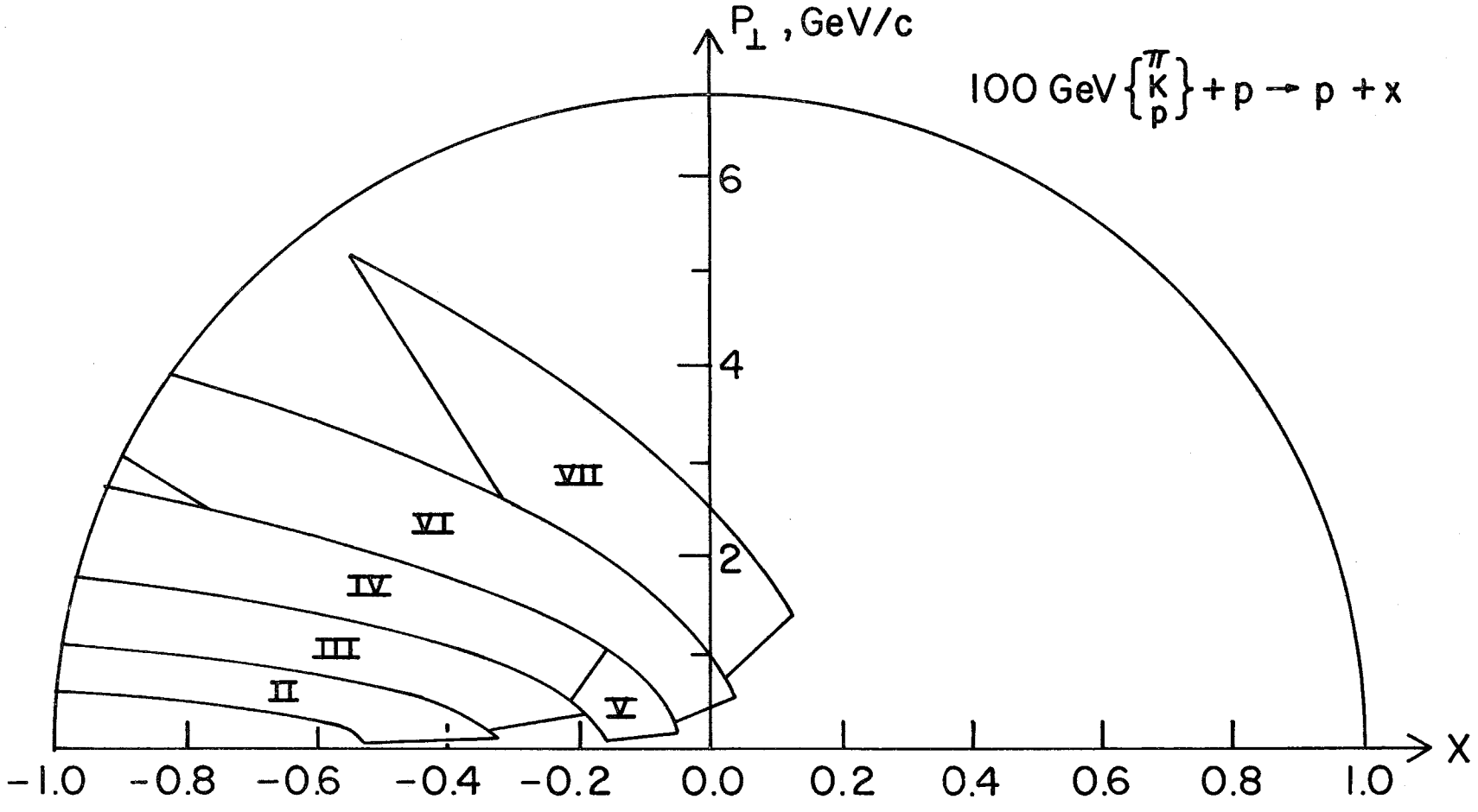

Figure 3. Peyrou plot showing the kinematic region covered in our experiment for the production of protons by 100 Gev pions, kaons or protons.

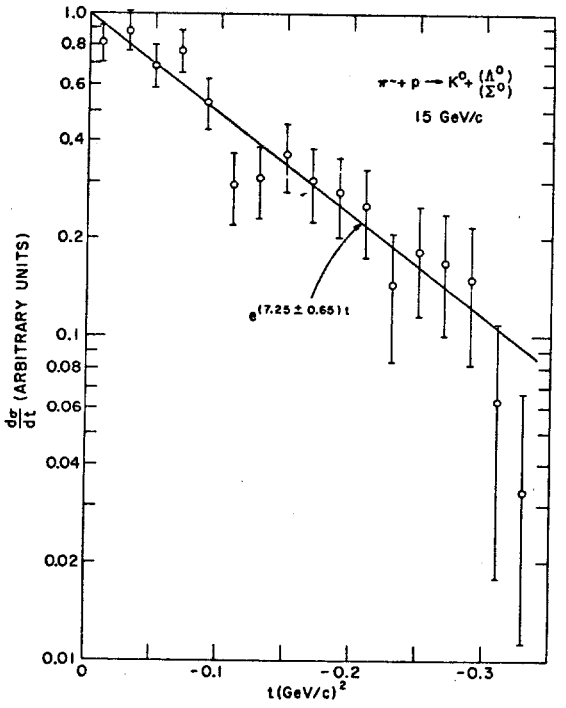

Figure 5: $\frac{d\sigma}{dt}$ versus -t for $\pi^- + p \rightarrow K^o + \begin{pmatrix}\Lambda\\ \Sigma\end{pmatrix}$. 15 GeV/c incident π^- were run for $\sim$ 10 hours under test beam conditions, in the first runs during the Spring of 1969.

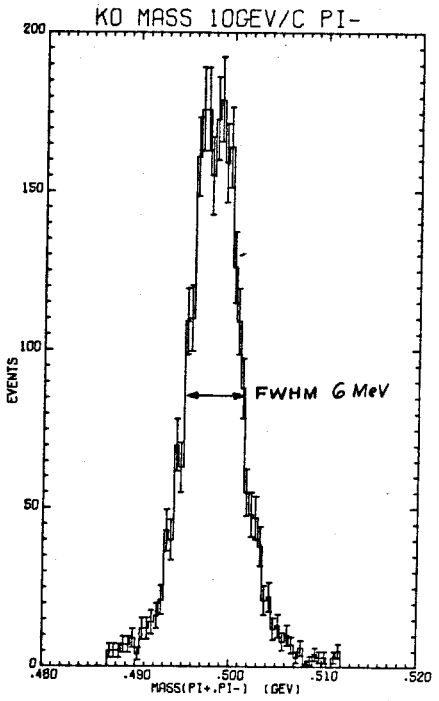

Figure 6: Reconstructed K^o mass spectrum in the forward Vee detecting arm for incident π^- particles in a short test run. The trigger arrangement used required that in fast coincidence, an incident π^- beam particle (identified by Cerenkov counters) apparently disappears in the hydrogen target and does not trigger the anti downstream of the hydrogen target, and particles trigger a counter before the magnet, and in fast coincidence two particles strike the two counter hodoscopes at the extreme downstream end. Typically, one trigger in ten turned out to be a true K^o event. This is the entire curve -- no background was subtracted, although the mass plot was limited within the limits shown, HWHM $\approx$ 3 MeV. Part of this is due to misalignments and non-uniformities in the magnetic field, which will be corrected for. The resultant estimated HWHM $\approx$ 2 MeV.

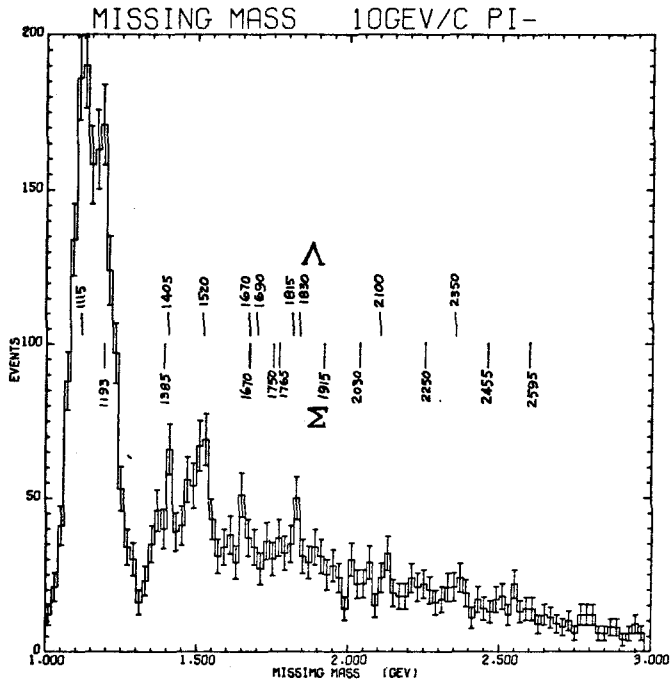

Figure 7: The missing mass spectrum corresponding to the K^o produced forward in the reaction $\pi^- + p \rightarrow K^o$ - - - - at 10 GeV/c. The location of known Λ and Σ states is also illustrated.

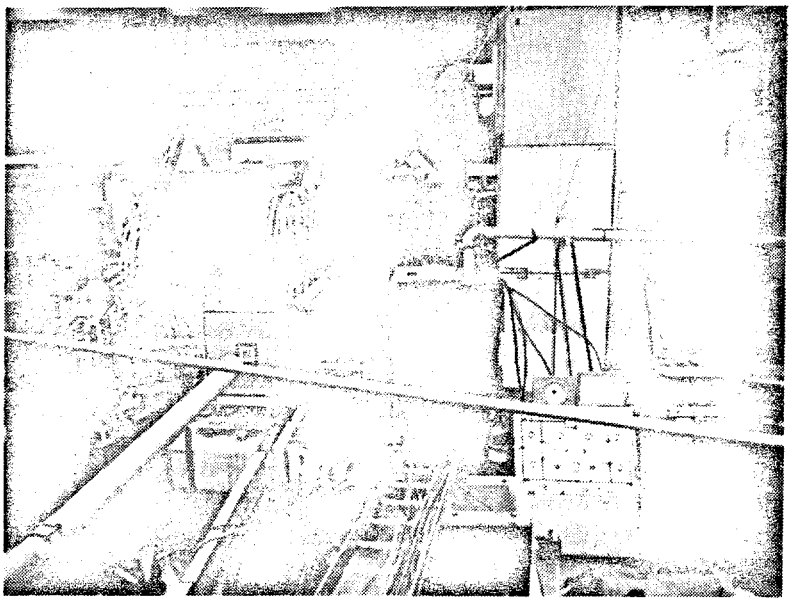

Figure 8: A photograph of the system as it stands at present. The beam enters from the left foreground through vacuum pipe, passes through the beam hodoscope and threshold Cerenkov counter, and then enters a two foot long hydrogen target. On the left side of the hydrogen target is the wide-angle Vee detecting arm of the spectrometer with spark chambers before and after the large (10' wide x 3' deep x 3' high) magnet. Downstream of the hydrogen target one can see the forward Vee detecting system already described in Figure 1.

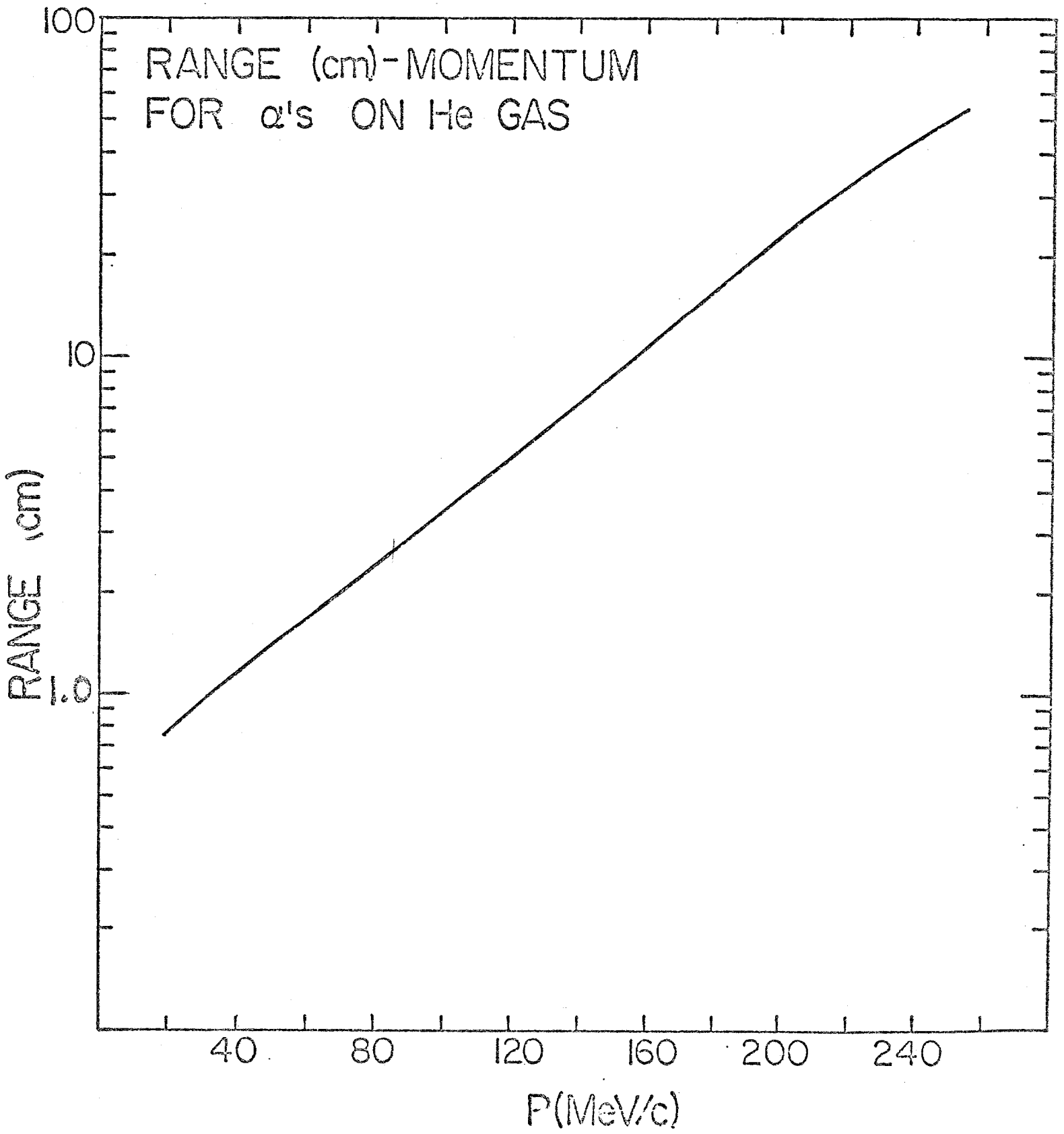

Figure 7, Range of He in He gas at 1 atmosphere.

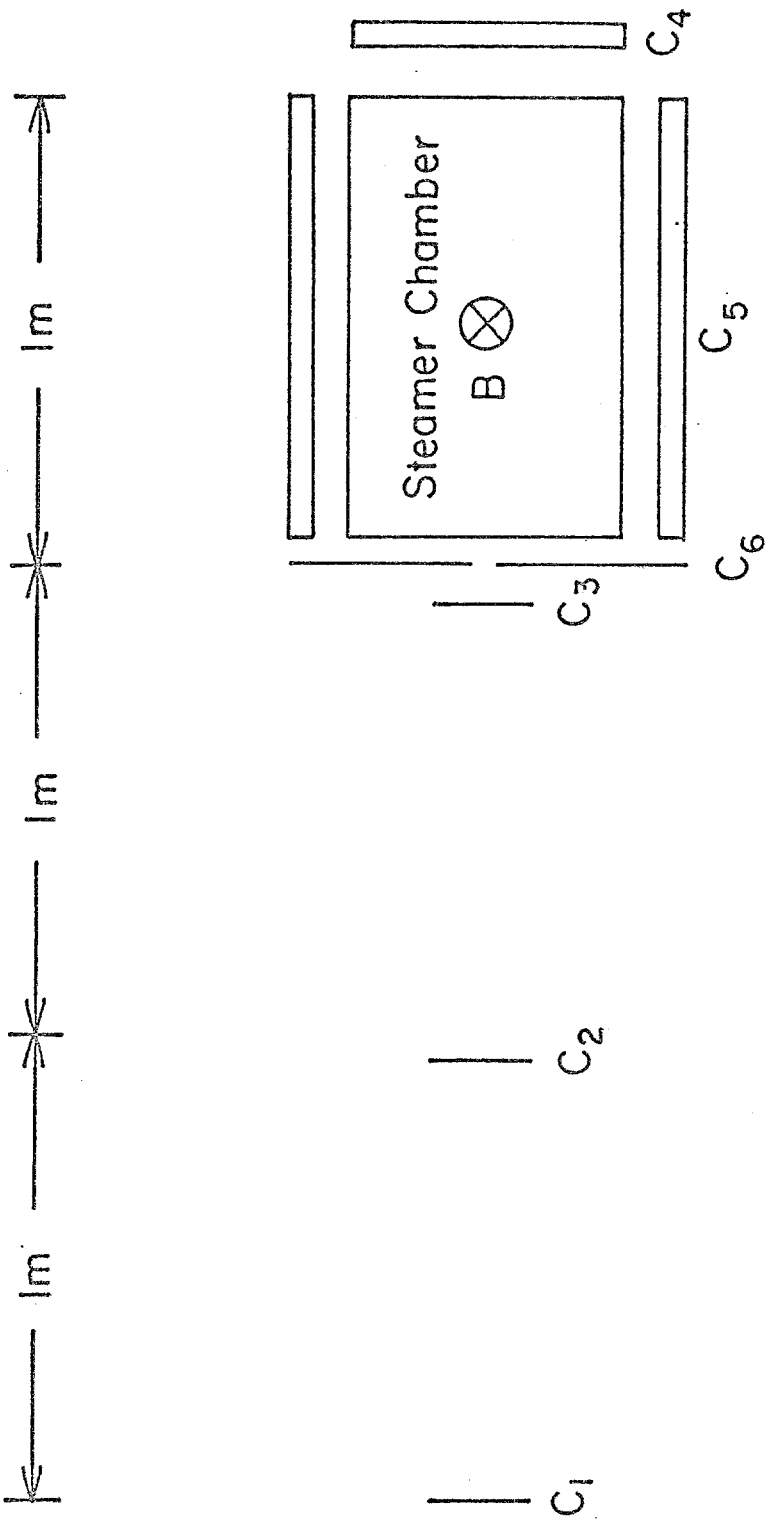

Figure 8a, Experimental Arrangement.

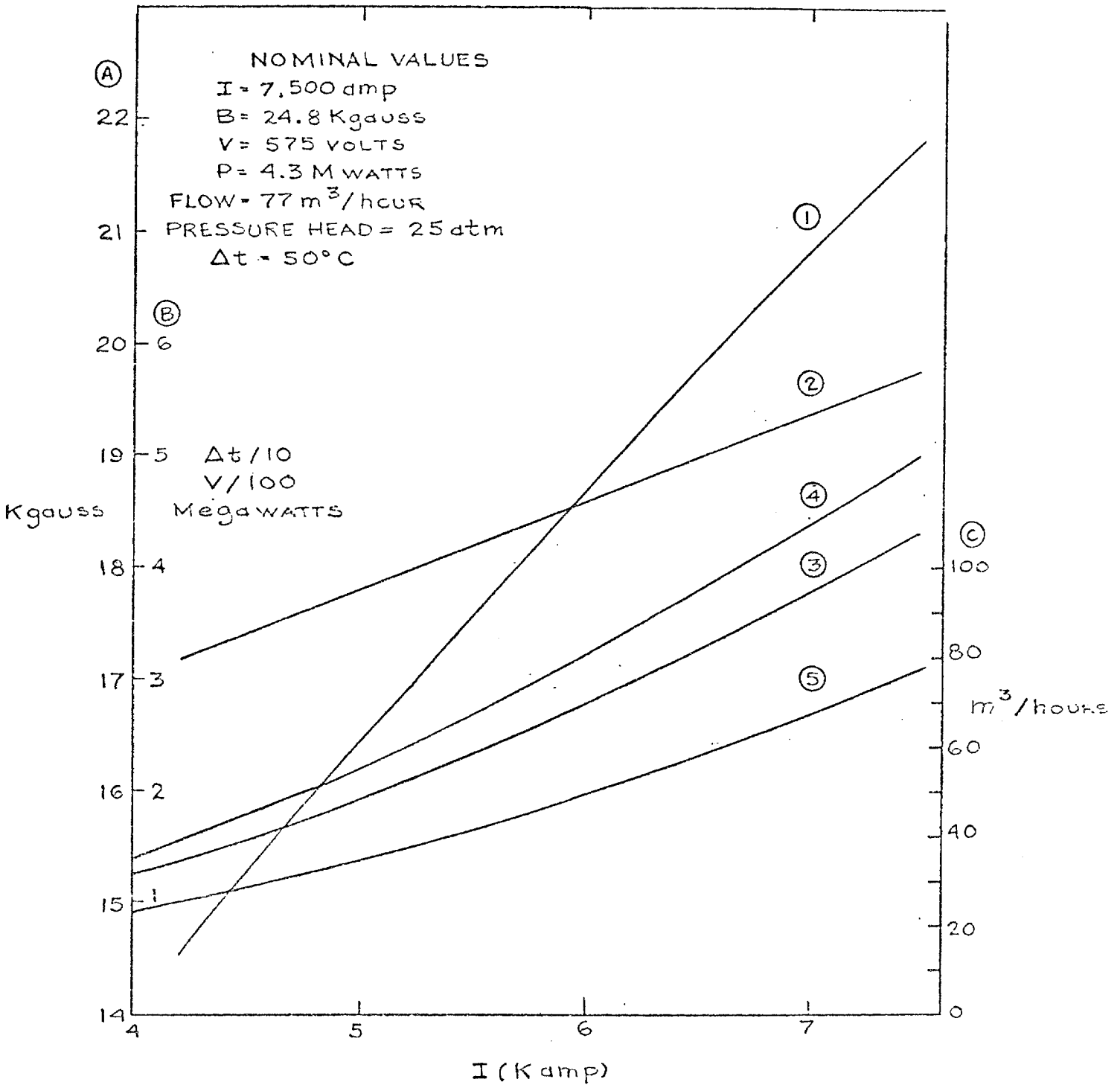

Figure 9 - Magnet Parameters

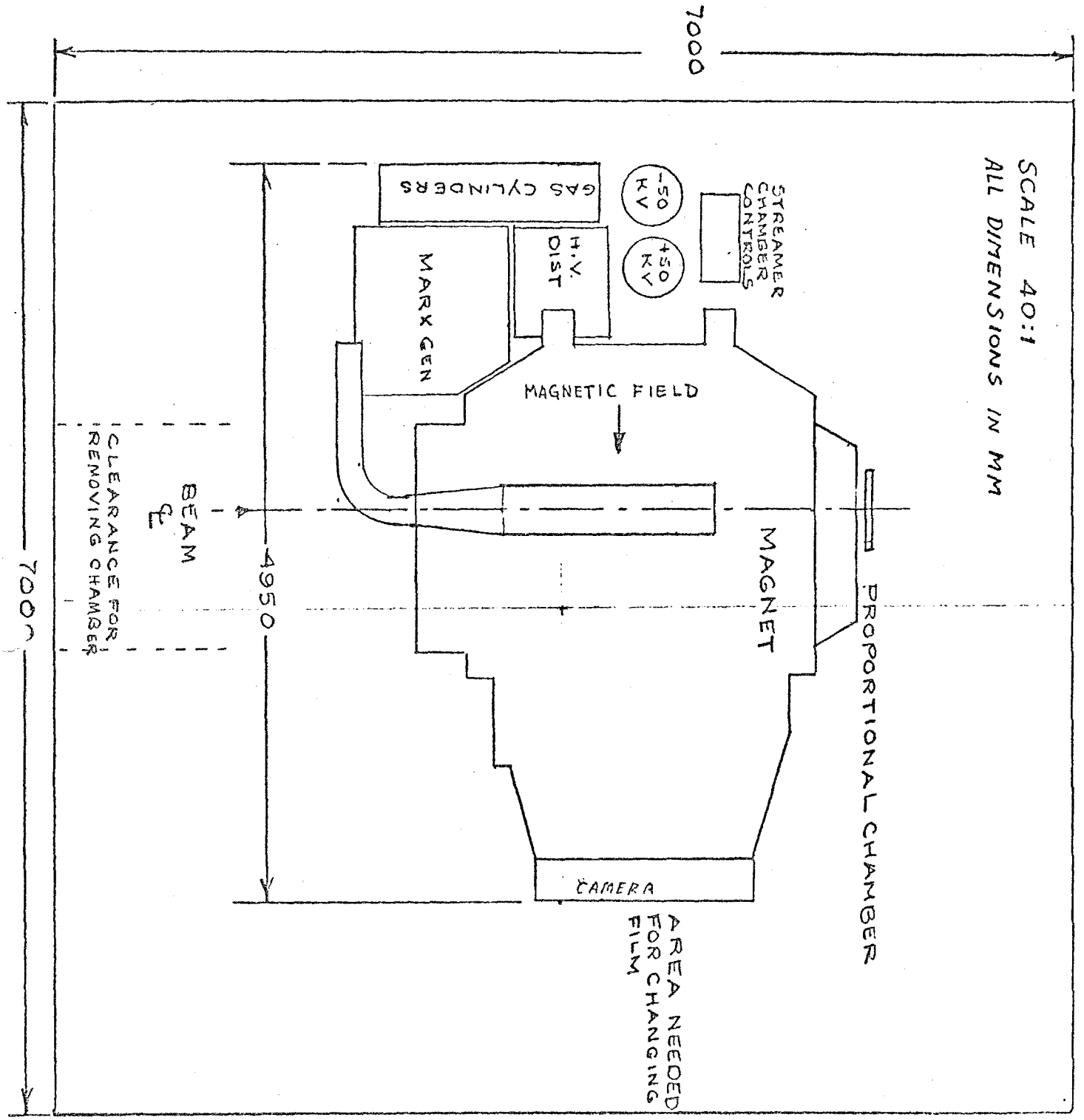

Figure 10, Top view of experimental layout - (Section taken through center of magnet)

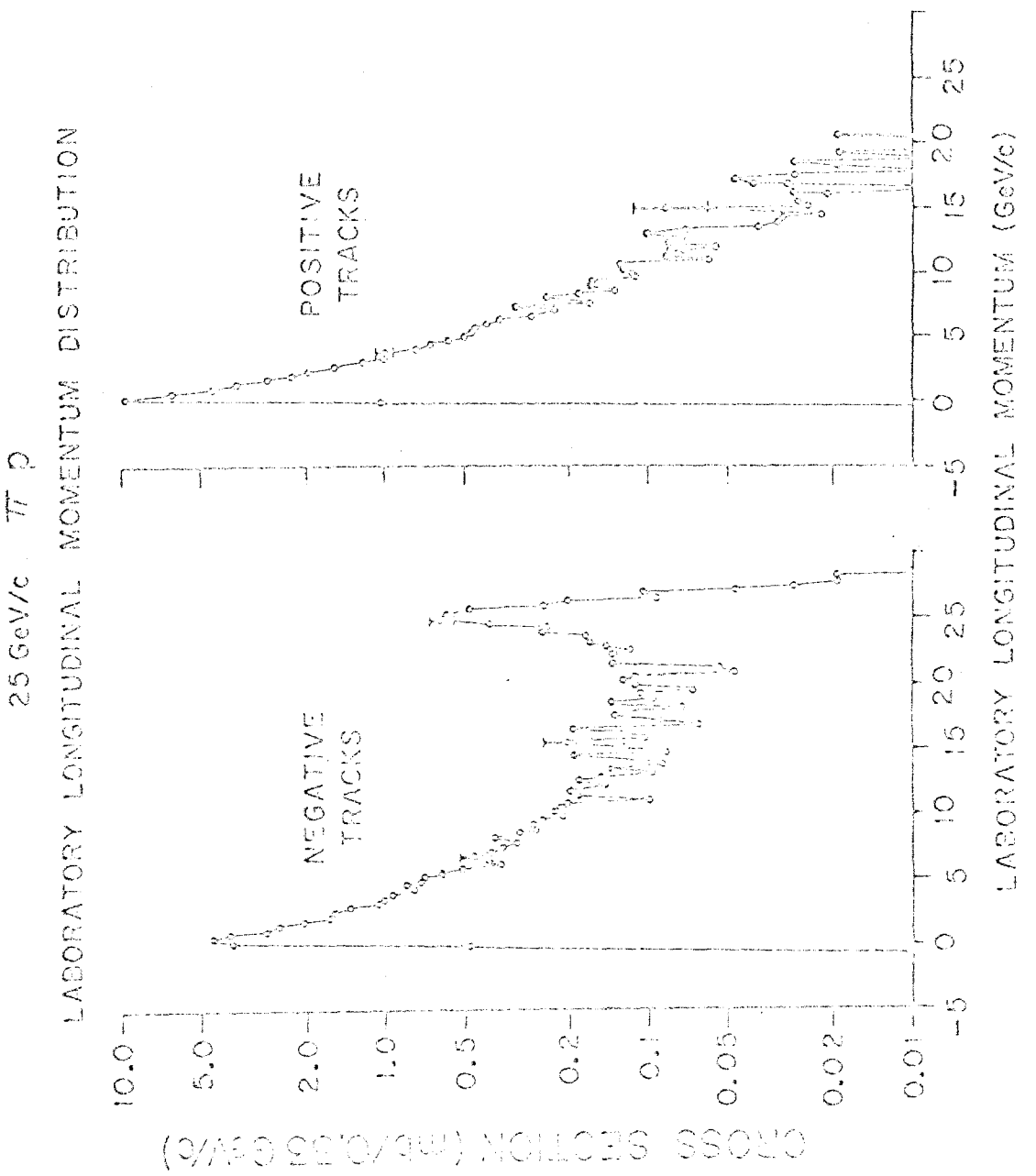
25 GeV/c $\pi^- p$
LABORATORY LONGITUDINAL MOMENTUM DISTRIBUTION
POSITIVE TRACKS
NEGATIVE TRACKS
CROSS SECTION (mb/0.05 GeV/c)
LABORATORY LONGITUDINAL MOMENTUM (GeV/c)
10.0
5.0
2.0
1.0
0.5
0.2
0.1
0.05
0.02
0.01
-5
0
5
10
15
20
25

FIG. 14

RECENT THEORETICAL DEVELOPMENTS ON INCLUSIVE DIFFRACTIVE PROCESSES

Addendum to Proposal #86

Spokesman: H. J. Lubatti

19 February 1971

SUMMARY

Recent unpublished theoretical developments by Abarbanel, Chew, Goldberger and Saunders at Princeton and DeTar, Jones, Low, Tan, Weis and Young at MIT have demonstrated the importance of studying diffraction dissociation in order to understand one of the most puzzling notions in the theory of strong interactions, namely the role of the vacuum or Pomeranchuk coupling. In this addendum we discuss the relation of these new theoretical developments to Experiment # 86 which proposes to study in a simple way diffraction dissociation of a hadron by using a helium nucleus as a target.

Recall that Experiment #86 plans to use the helium streamer chamber as a "living target"; that is, the helium gas in the chamber serves as a target as well as a detector of the recoiling helium nucleus. Measurement of momentum and angle of the recoiling helium in the chamber allows us to calculate the missing mass of the dissociated hadron system. In the original proposal we stress the significance of studying the states into which a pion dissociates. We still feel that it is an important part of our experiment; however, what we wish to discuss in this addendum is a slightly different region of the missing mass spectrum which we obtain automatically: namely, the high missing mass region where there should be no resonant structure. It is this region which the above theorists have studied in great detail. In particular they have found that the interesting quantity to measure is the differential cross section $d\sigma/dtds'$ for the inclusive reaction $\pi + He \rightarrow anything + He$, where s' is the mass squared of the hadron system labeled above by "anything".

We emphasize that these new theoretical ideas involve data in a kinematic region that was already covered in the experiment already proposed. Therefore, we are not discussing any change in the experimental apparatus or running time, but rather the heightened interest in a part of the data we shall obtain. In fact, the inclusive cross section is the easiest part of the experiment to analyze, since it does not require any information about the multiplicity of the fast particles. We need only measure the He recoil and calculate a missing mass.

In the following we discuss the importance of diffraction dissociation and summarize the new theoretical developments.

DETAILED DISCUSSION

Diffractive processes, which have long played a prominent role in elementary particle physics are the most simple processes to study, but at the same time they are among the most difficult and challenging phenomena which we have encountered. In attempting to explain such phenomena in terms of exchange models, we have been forced to the concept of the vacuum exchange or, in the Regge model language, the exchange of the Pomeranchuk trajectory. Such a concept, while preserving the basic ideas inherent in the exchange model, presents some difficulties. The chief problem has been that while other trajectories all have known particles lying on them, there has not yet been observed a particle which unambiguously can be associated with the Pomeranchuk trajectory. In addition, the original conjecture that $\alpha_{\text{Pomeron}}(0)$ is equal to 1, never has been adequately tested in the energy range available at existing accelerators.

Experimentally, we can define a diffractive process as one in which no internal quantum numbers (B,Y,T,G,and $\sigma = (-1)^{J}P$) are exchanged. This simply means that for the process $1 + 2 \rightarrow 3 + 4$ particle, 1(2) and 3(4) have the same internal quantum numbers. Elastic scattering is an obvious example of such a process. Another example of such a process is $p + p \rightarrow p + N^{*}$, where the N^{*}'s are the $T = \frac{1}{2}$ isobars. Another example which has been observed is the production of the A_1 and Q mesons. All of the data which have been obtained at existing accelerator energies have merely served to wet our appetite about the true nature of the diffractive process. The amazing result that an inelastic diffractive cross section remains constant with energy suggests that at NAL energies diffraction dissociation should become an important if not the most important phenomenon in strong interactions.

Recent theoretical work by Chew, Abarbanel, Goldberger and Saunders at Princeton [1], and DeTar, Jones, Low, Tan, Young and Weis [2] at MIT has given considerable insight into the question of diffraction dissociation. The crucial observation of the Princeton group has been that in order to better understand the vacuum coupling one

should study inclusive diffraction dissociation reactions, and not quasi-two-body processes. The importance of this observation is greatly enhanced by the fact that experimentally it is much simplier to study inclusive reactions than it is to try to pick out specific quasi-two-body channels. Now, in fact, we know that all of the quasi-two-body production data which we have accumulated in the past ten years has served only as an indication that there is validity to the exchange model, but has not given us any profound insight into the theory of strong interactions. What we have learned is that at higher energies quasi-two-body processes become less important because of the $1/s^n$ dependence; with the exception, of course, of those processes which are diffractive.

The particular theoretical process which has been studied in detail by the Princeton theorists has been A + target → anything + target, where A is a high energy hadron. The only requirement for the target is that it simply take up the recoil momentum necessary for conservation of energy when the incident particle changes its mass to some effective $M^2 \equiv s'$. Diagrammatically, this is demonstrated in Figure 1. Since precisely this process is mediated by the Pomeron exchange, it is quite obvious that a detailed study of such a process will serve as a test for any theoretical model which purports to study diffractive processes. The Princeton theorists have

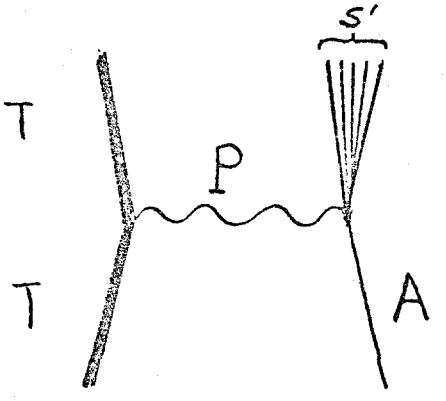

Figure 1

been able to relate this process to a fundamental notion in the theory of strong interactions, namely that of the three Pomeranchuk vertex. Such ideas have also been discussed by Gribov [3] and others, but the more recent work of Abarbanel, Chew, Goldberger and Saunders [1] makes explicit statements about what one should expect from such inclusive reactions and their profound relevance to the theory of strong interactions. The salient result found by these workers is that the inclusive diffraction dissociation cross section at large missing masses (i.e., large s' in Figure 1) is proportional to $\sqrt{1 - \alpha_P(0)}$. Therefore, in this experiment where we are measuring the cross section for the reaction π + He → anything + He, we are measuring $\alpha_P(0)$. It is this fact which I have referred to as an amazing discovery because heretofore the only way we thought we could learn something about the intercept of the Pomeron at t = 0 was to study the energy dependence of the total cross sections, and since we expect that $1 - \alpha_P(0)$ is of the order of 0.01 or smaller, we would have to observe an energy dependence of the total cross sections which goes as $1/s^{(0.01)}$. Needless to say, such an experiment would require extraordinarily precise cross section measurements with extremely fine granularity in energy; however, since in the inclusive π + He reaction we measure the square root of $1 - \alpha_P(0)$; a 1% effect in the total cross section becomes a 10% effect in this experiment. In the following we give a summary of the relevant formalism developed by the Princeton group.

The theoretical developments alluded to above have demonstrated that in the collision shown in Figure 1, taking target ≡ He and A ≡ π, the cross section can be asymptotically represented by

$$s^2 \frac{d\sigma}{ds'dt}\left(s', \underset{\text{large}}{\sim} s/s'\right) \frac{1}{16\pi} \left|\beta_{HeP}(t)\right|^2 \beta_{\pi P}(0) g_{PPP}(t) (s')^{\alpha_P(0)} \left(\frac{s}{s'}\right)^{2\alpha_P(t)} . \quad (1)$$

The normalization of the vertex factors is such that π + He → π + He has the asymptotic form

$$s^2 \frac{d\sigma^{el}_{\pi He}}{dt} \underset{s \text{ large}}{\sim} \frac{1}{16\pi} \left|\beta_{HeP}(t)\right|^2 \left|\beta_{\pi P}(t)\right|^2 s^{2\alpha_P(t)} \quad (2)$$

The quantity $g_{PPP}(t)$ is the triple Pomeranchuk vertex function, and it is this quantity which Chew feels is of central importance in the theory of strong interactions [1]. In particular, the Princeton theorists show that

$$\eta_P \equiv \frac{1}{16\pi}\frac{1}{2\alpha'(0)}\left[g_{PPP}(0)\right]^2 \leq 1 - \alpha_P(0) \ . \tag{3}$$

If we integrate over t and then normalize Eq. (1) to the elastic cross section Eq. (2), we find the following relationships

$$\frac{1}{\sigma^{el}}\frac{d\sigma}{d\ln s'}\left(s', \tilde{s}/s'\right)_{\text{large}} \simeq \frac{g_{PPP}(0)}{\sqrt{\sigma_{\pi\pi}}} = \sqrt{\frac{16\pi(2\alpha')\eta_P}{\sigma_{\pi\pi}}} \ . \tag{4}$$

Therefore, we can estimate the experimental effect we would observe by taking η_P to be of the order of 0.01 and $\alpha' \simeq \frac{1}{2}$; $\sigma_{\pi\pi}$ is known to be approximately 15 mb. We find that

$$\frac{1}{\sigma^{el}}\frac{d\sigma}{d\ln s'} \simeq 0.1 \tag{5}$$

We have also calculated, using the Glauber model, the elastic π He cross section to be about 11 mb at 100 GeV/c; hence, we expect $d\sigma/d\ln s'$ to be of the order of 1 mb, which is easily detectable in our experiment. In fact, in our recent supplement to the proposal, which delt with triggering rates, we estimated conservatively the total π He coherent production cross section to be 3 mb. Thus, the result in Eq. (5) is not unreasonable, since our 3 mb estimate also included resonant structure in the s' mass distribution. What Chew and coworkers are calculating is applicable to large s' where the resonant structure has damped out.

Note that if $g_{PPP}(0) = 0$ then we would observe a decrease of (or absence?) of events at large s'. This, in itself, would be an important discovery. For example such a result would exclude certain proposals which have been made about the Pomeranchuk trajectory [4].

Even more significant will be a study $g_{PPP}(t)$ as a function of t. We will be able to measure the momentum of the He recoil to approximately 2 MeV/c (recall that the He stops in the chamber), and hence we will have precise momentum transfer distributions at small values of t.

We remind the reader that the above theoretical predictions apply only to the region of large s'. In the resonance region (small s') we will apply the analysis we have discussed in detail in the proposal.

It is to be noted that because the above theoretical arguments stress small momentum transfers, the nuclear form factor which restricts us to small t values makes the nucleus a better target than a nucleon. For example, we expect the He form factor to give us approximately an e^{40t} dependence in momentum transfer, while a nucleon gives an e^{10t} dependence. Another important point is that the above arguments do not depend on the exact nature of the incident particle, only that it be a hadron. Hence, protons will be as interesting as pions, and the final choice of beam particle should best be left to the convenience of the scheduling committee, although we confess to having a historical preference for pions.

In conclusion, this simple experiment measures a profoundly important quantity, namely the diffraction dissociation cross section of a hadron dissociating into anything. This cross section has already been related to η_p which measures the strength of the three Pomeron coupling which in turn is related to the intercept of the Pomeranchuk trajectory at t = 0, and is therefore a parameter of central importance in the theory of strong interactions. Because such measurements require that both s and s/s' be large, it is necessary to perform these experiments at NAL. We stress once more the enormous role which diffractive processes play in the understanding of strong interactions. Therefore, we feel that an experiment which is simple in nature and can give results which are relevant to new, exciting theoretical ideas should be done as soon as possible.

References

1) Private communication from G. F.Chew. At present these results exist only in handwritten manuscript; however, Chew has offered to discuss this with the NAL committee if necessary.

2) C.E. DeTar, C.E. Jones, F.E. Low, J.H. Weis, J.E. Young and Chung-I Tan, "Helicity Poles, Triple Regge Behavior and Single Particle Spectra in High Energy Collisions". MIT Preprint.

3) V.N. Gribov and A.A. Migdal, Sov. J. Nucl. Phys. 8, 1002 (1968). V.N. Gribov and A.A. Migdal, Sov. Phys.—JETP, 28, 784 (1968).

4) G.F. Chew and D. Snider to be published, and private communication G.F. Chew.

REQUEST FOR RECONSIDERATION OF NAL PROPOSAL 52

(SINGLE PARTICLE INCLUSIVE SPECTRA IN $\left\{\begin{matrix}\pi^{\pm}\\ k^{\pm}\\ p\end{matrix}\right\}$ + p → $\left\{\begin{matrix}\pi^{\pm}\\ k^{\pm}\\ p^{\pm}\end{matrix}\right\}$ + anything)

Experimenters: E. W. Beier, H. Brody, K. Raychaudhuri, H. Takeda
R. Thern, R. Van Berg, H. Weisberg

Physics Department
University of Pennsylvania
Philadelphia, Penna. 19174

Date: March 1974

Correspondent: H. Weisberg (Telephone 215-594-6481 FTS/COMM)

Request for Reconsideration of NAL Proposal 52

(Single Particle Inclusive Spectra in $\begin{Bmatrix} \pi^{\pm} \\ k^{\pm} \\ p^{\pm} \end{Bmatrix}$ + p → $\begin{Bmatrix} \pi^{\pm} \\ k^{\pm} \\ p^{\pm} \end{Bmatrix}$ + anything)

Experimenters: E. W. Beier, H. Brody, K. Raychaudhuri, H. Takeda, R. Thern, R. Van Berg, H. Weisberg

Physics Department
University of Pennsylvania
Philadelphia, Penna. 19174

Date: March 1974

Correspondent: H. Weisberg (Telephone 215-594-6481 FTS/COMM)

ABSTRACT

We resubmit our proposal to measure the differential cross section for the production of particle c in the single-particle inclusive reaction a + b → c + anything, where a and c are any combination of $\pi^{\pm}$, $k^{\pm}$ and $p^{\pm}$. Spectra will be measured with incident momenta P_a = 40, 80 and 160 Gev/c over a range of secondary momenta P_c = 0.3 - 2.5 Gev/c and angle θ_c = 5 - 180°, covering the target fragmentation region and part of the central region. In addition we will make precision measurements of the s-dependence of the inclusive cross-sections integrated over the fixed range P_c = 0.3 - 0.6 Gev/c and θ_c = 53 - 57°, for six incident momenta extending to the highest available in the Meson Area. The cross-sections will be measured with the U. of Pa. Single Particle Spectrometer, which is presently being used at the Brookhaven A.G.S. Preliminary A.G.S. results are presented to document the performance of this spectrometer.

INTRODUCTION

There are three principal reasons for reconsideration of this proposal:

(1) We have now completed the 0.25 - 2.5 Gev/c secondary momentum phase ("short arm") of our BNL running and can document the quality of our spectrometer with actual data.

(2) Based on our running experience at BNL, we have modified our proposal somewhat. First, we have added a series of precision s-dependence measurements with fixed spectrometer momentum and angle and variable beam momentum. These will extend our A.G.S. s-dependence measurements, preliminary results of which are presented below. Second, we have decided to measure spectra with the short arm only. This still gives complete coverage of the target fragmentation kinematic region, but it gives only partial coverage of the central region. The kinematic region from 2.5 Gev/c, where the short arm coverage stops, to 20 Gev/c, where the SAS facility begins its coverage, can be studied with our "long arm" configuration. We leave this for a future proposal.

(3) We understand that the University of Washington group has shifted its interest from inclusive scattering to hadron jets, and that their inclusive scattering experiment has been taken off the schedule. These is now a large gap in the physics of the NAL program: specifically, there is no precision measurement of inclusive spectra in the target fragmentation and central region, with incident particles other than protons.

Part I of this document is an updated summary of our proposal. Part II is a preliminary report on our inclusive scattering results at BNL. Part II is in response to Prof. Wilson's letter at the time our proposal was initally deferred. That letter stated that action on our proposal would be deferred until preliminary results from our work at Brookhaven became available.

I. SUMMARY OF PROPOSAL

Physics

With the construction of the CERN ISR and the NAL 400 GeV synchrotron, an understanding of multiparticle production processes in hadronic interactions has assumed a role of fundamental importance. Although the general features of these processes has emerged, the data are, in many cases, meager, and experiments performed at different energies with different techniques are often difficult to compare because of restricted kinematic coverage, relative normalization errors, etc. Thus, there exists no set of measurements which fully test the content of models such as the Mueller-Regge phenomenology; for example, factorization, the approach to scaling, production by π's and k's, and so forth. We believe the measurements we propose are as important as measurements of total and elastic cross sections and should be performed at NAL early in the accelerator program.

We propose to extend our systematic study of single particle production, begun at the Brookhaven AGS, to NAL energies. Specifically we propose to measure the differential cross section for the production of particle c in the single particle inclusive reaction:

$$a + p \rightarrow c + \text{anything}$$

where a and c are any of the charged hadrons $\pi^{\pm}$, $k^{\pm}$ and $p^{\pm}$. We sometimes shall abbreviate this reaction as " a → c".

The measurements we propose are of two types. The first type is a measurement of the spectrum of particle c for

$$x = \frac{P_{11}^{cm}}{P_{11}^{cm}\ (MAX)}$$

in the interval $-1.0 < x \leq 0.0$ at incident laboratory momenta P_a = 40, 80, and 160 GeV/c. Our spectrometer provides continuous coverage in secondary lab momentum and lab angle and therefore does not prejudice the measurement in favor of any particular set of variables. Together with our existing AGS measurements at 8, 12, and 20 GeV/c, these higher energy measurements will provide a consistent set of cross sections over a large range of center mass energy.

The second type of measurement is a precision determination of the s-dependence of the inclusive cross-section integrated over the fixed range P_c = 0.3 - 0.6 Gev/c, θ_c = 53 - 57°, i.e at a single fixed spectrometer setting. These s-dependence measurements will be made with six incident momenta ranging from 20 Gev/c up to the highest available at the Meson Lab. They will supplement our AGS measurements at 4, 6, 8, 10, 12, 15 and 20 Gev/c.

Spectrometer

The University of Pennsylvania Single Particle Spectrometer (Fig. 1) is fully operational at the AGS and requires no further development. The spectrometer is constructed on a steel arm which rotates about a pivot beneath a liquid hydrogen target. A small C-magnet (12C24 with 4" gap) is used in conjunction with multiwire proportional counters (MWPC) and trigger scintillation counters to measure the differential cross section for production of charged particles in a given momentum interval. Immediately behind these detectors is a set of threshold Cerenkov counters, scintillation counters, and another MWPC which are used to measure the ratios of the particle types.

The spectrometer angle is varied in steps corresponding to about one third of the spectrometer's angular acceptance so that the cross section at each production angle is measured in different parts of the spectrometer. A "run" at fixed angle lasts about five minutes. A PDP-9 computer ends the run at a preset count, moves the spectrometer to the next angle, and begins the next run. Incrementing the spectrometer angle takes about six seconds and is accurate to one percent of the increment (the absolute angle is recorded).

The momentum acceptance is $\frac{P(MAX)}{P(MIN)} = 2$, and the momentum range 0.3 - 2.5 GeV/c is covered in three "configurations" of the spectrometer. The configurations have different particle identification detectors, magnet current, and MWPC transverse position. Changing between configurations is a simple procedure; each change is performed only once during the experiment.

The momentum resolution is typically $\frac{\delta P}{P} = .01$ rms. It is limited at low momentum by multiple scattering and at high momentum by the 2 mm wire spacing of the MWPC's.

Particle identification is achieved by the use of threshold Cerenkov counters, and, at low momentum, time of flight and energy loss. Typically, three Cerenkov counters are used. They identify π's, high momentum K's, and low momentum K's respectively. Although construction of counters with the specifications of some of the counters is non-trivial, the counters have been developed and used successfully at the AGS.

Running time and Schedule

The running time required is based on our experience at BNL and is:

1)	Measurement of spectrum	750 hours
2)	Measurement of s-dependence	250 hours
	Total	1000 hours

The equipment is constructed and running at BNL. We will be able to set up at NAL beginning Fall 1974.

We propose to perform the experiment in the west branch of the M1 beam. The entire spectrometer will fit in the alcove presently occupied by the target for Experiment #104 (Total Cross Section).

II. PRELIMINARY A.G.S. RESULTS

Normalization Accuracy

We have strived for absolute normalization accuracy at the few percent level. To search for rate dependent effects, we studied, as a function of incident intensity, the ratio R = (reconstructed secondaries)/(incident beam particles). The measured cross-section is directly proportional to this ratio. The data, Fig. 2, show no significant rate dependence.

In an analogous way we studied the dependence of R on horizontal beam steering. The data are shown in Fig. 3. When the beam is grossly mis-steered, the target full ratio increases because part of the beam hits the target walls, but the full-empty difference remains constant.

.To test the absolute normalization accuracy, we measured $\frac{d\sigma}{dt}$ for elastic scattering of π^+, π^- and p on protons at energies where prior measurements exist. A typical result is shown in Fig. 4. These measurements give us good confidence in our overall normalization.

Particle Identification

The spectrometer is designed for good secondary particle identification not only for $\pi^{\pm}$ and p, but also for $k^{\pm}$ and $\bar{p}$. Figures 5 a-b illustrate the mass separation for positive secondaries in the range P_c = 1.2 - 2.5 Gev/c, θ_c = 9-25°, which is near x = 0 for π's and k's. Fig. 5a is the pulse height spectrum for all secondaries going thru $\check{C}_1$, which separates π's from heavier particles. Fig. 5b is the pulse height spectrum in $\check{C}_3$, which separates low momentum k's from p's. Entries are made in this distribution only for particles with P_c = 1.2 - 1.88 Gev/c and $\check{C}_1$ pulse height below 160, i.e. low momentum k's and p's.

In general it appears that uncertainties due to π/k/p misidentification are small throughout our data.

Spectra

We have measured inelastic spectra at P_a = 8, 12 and 20 Gev/c, P_c = 0.3 - 2.5 Gev/c, and θ_c = 5 - 180°, with all four polarity combinations. These data have not yet been reduced, but the systematic checks described above give us good confidence in our measurements. Approximately 5×10^6 good events have been recorded.

s-Dependence

We have also measured the s-dependence of the inclusive cross-sections at a fixed secondary momentum in the lab corresponding to the target fragmentation region. These data have been analyzed up to an overall normalization constant, and preliminary results are presented in Fig. 6. The points plotted give values of the inclusive cross-section, integrated over the fixed spectrometer acceptance, in arbitrary units, for various beam momenta (s values). Relative normalization is all that is needed to study the s-dependence of these data; absolute normalization will be obtained later.

There are several aspects of these data that suggest that extension to NAL energies will be particularly profitable.

(1) Accuracy

For the nine copious reactions $\{\pi^{\pm}, p\} \rightarrow \{\pi^{\pm}, p\}$, statistical accuracies approaching 1% are obtained and there appear not to be any s-dependent normalization problems. This is to be compared with normalization discrepencies of ~10% which are encountered in comparing inclusive scattering measurements with bubble chambers.

(2) Limiting Behavior and Pomeron Factorization

It is widely believed that:

(a) inclusive cross-sections of the type we have measured approach a high-energy limit;

(b) the approach to the limit has the form $A + Bs^{-1/2}$;

(c) the high-energy limit is the same for particle and antiparticle in the beam;

(d) the limits of the cross section at $s = \infty$ for different beam particle types are in the same ratio as the corresponding total cross-sections (Pomeron factorization)

Our data are roughly (to within a factor of ≤ 1.5) compatible with these features. However we are unable to fit our data in detail with models satisfying (a) - (d). For example in the simple Mueller-Regge pole model Pomeron factorization requires the intercepts for $\{p \to \pi^-\}$ and $\{\pi \to \pi^-\}$ at $s = \infty$ to have the same ratio as the total pp cross section and the total πp cross section at $s = \infty$. Our data suggest violation of Pomeron factorization by 20% in $\{\pi^\pm, p\} \to \pi^+$ and 40% in $\{\pi^\pm, p\} \to \pi^-$. These results are suggestive but not definitive. Clearly, measurements at higher energies are needed to provide a definitive answer. The question of Pomeron factorization is of fundamental importance to an understanding of high energy hadronic interactions; our kind of measurement is one of the few experimentally feasible direct tests.

(3) The Approach to Scaling

There is a type of information which can come essentially from our AGS data alone: by assuming that the high energy behavior is at least crudely given by (2a-d) above, we obtain information about the rate of approach to scaling. The results are in the form of B values in $A + Bs^{-1/2}$ for the fifteen reactions $\{\pi^\pm, k^\pm, p^\pm\} \to \pi^\pm$ and $\{\pi^\pm, p\} \to k^+$.

The values obtained are insensitive to the details of the high energy behavior assumed. We find clear contradictions with certain of the predictions which have been made about the approach to the scaling limit using duality. For example note the strong s-dependence of $p \rightarrow \pi^{\pm}$ (Figs. 6 a,b) which according to common folklore scales early.

It is obvious that the approach to scaling needs further study at NAL. The extended s interval will give a better lever arm for the slope determinations. Because of the favorable $\bar{p}$ and k fraction in the NAL beam, we will be able to study k^+ and k^- induced reactions with good statistics, and $\bar{p}$ induced reactions with moderate statistics. Finally, we should be able to study proton production in the Regge region (our AGS proton production data correspond to missing masses in the resonance region; Regge behavior may be setting in at our highest s-values (Figs. 6 i-k).

(4) Analogy with Total Cross-Section Measurements

The physics of our s-dependence measurements is similar to that of total cross-section measurements. Therefore, one of the exciting possibilities is that there may be unexpected deviations from simple extrapolations, analogous to those seen in total cross section measurements at Serpukhov and, more recently at the ISR.

FIGURE CAPTIONS

Fig. 1. Plan view of the "short arm" spectrometer, which measures angle, momentum and particle type from 0.3 to 2.5 Gev/c. Mounted on the rotary carriage are a 12C24 magnet, trigger counter T_{1-3}, proportional wire chambers PC_{1-5} and threshold Čerenkov Counters $\check{C}_{1-3}$.

Fig. 2. Rate dependence of the measured cross-section. The normal operating beam rate ranges from 0.1×10^6 particles/pulse at the smallest spectrometer angles to 1.5×10^6 at large angles.

Fig. 3. Beam steering dependence of the measured cross-section. In normal operation the magnet is kept within the limits marked "DVM Tolerance".

Fig. 4. Elastic calibration. The cross-section $\frac{d\sigma}{dt}$ for $\pi^- p$ elastic scattering as measured in this experiment is compared with previous measurements.

Fig. 5. Spectrometer Čerenkov counter pulse height distribution for a sample of 50% of the data for 20 Gev/c positive beam and 1.2 - 2.5 Gev/c, 9-25 degree positive secondaries.

(a) Spectrum for $\check{C}_1$, which operates at an index of refraction n = 1.019 in order to count π's but not k's and p's.

(b) Spectrum in $\check{C}_3$, which operates at n = 1.117. Only particles of momentum 1.2 - 1.88 Gev/c and pulse height below 160 in $\check{C}_1$ are entered in this distribution, which therefore contains essentially p's and k's only.

Fig. 6. Preliminary s-dependence results. These are raw data on the number of events detected in fixed spectrometer acceptance near P_c = 0.3-0.6, θ_c = 53° - 57°, per 10^8 beam particles. The following important corrections

have not been applied: π and K decay and interactions; spectrometer acceptance variation; lepton contamination in the beam. All but the last of these corrections are expected to be roughly s-independent. Lepton contamination may be important at low s, but has not been measured yet.

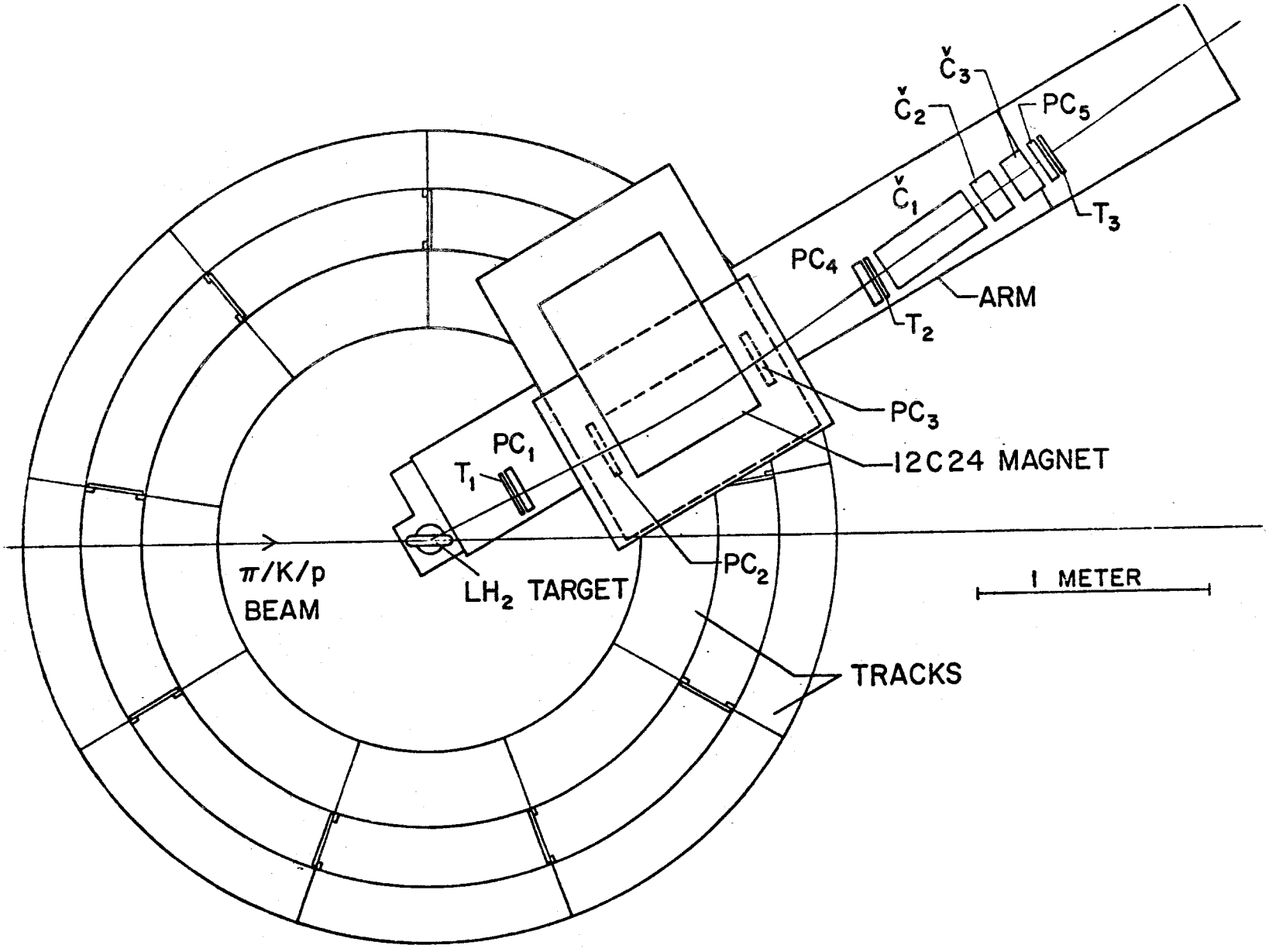
$\check{C}_3$
$\check{C}_2$
PC_5
$\check{C}_1$
T_3
PC_4
ARM
T_2
PC_3
PC_1
T_1
12C24 MAGNET
π/K/p
BEAM
LH_2 TARGET
PC_2
1 METER
TRACKS

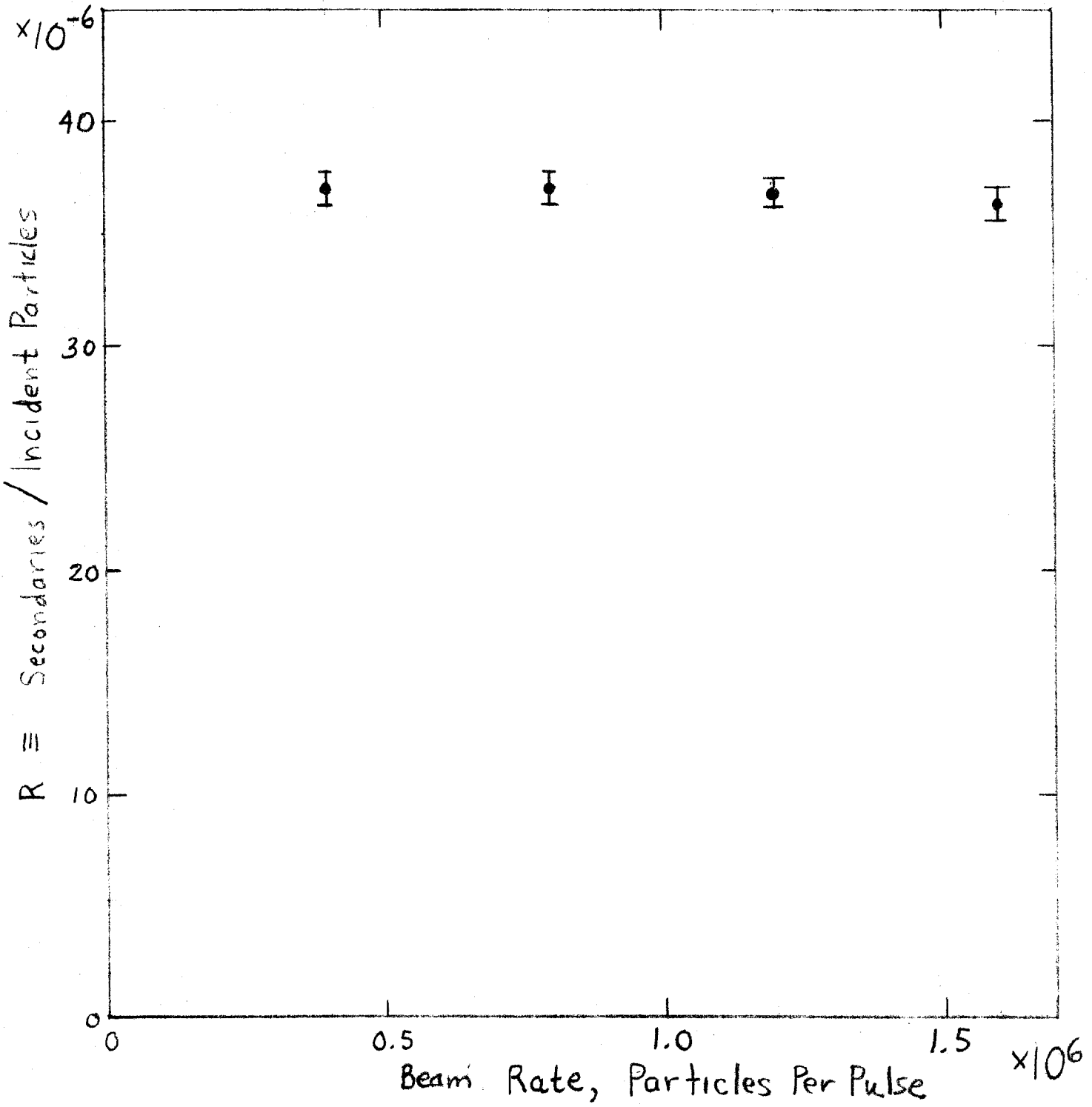
×10⁻⁶
40
30
20
10
0
R ≡ Secondaries / Incident Particles
0
0.5
1.0
1.5
×10⁶
Beam Rate, Particles Per Pulse

Figure 2

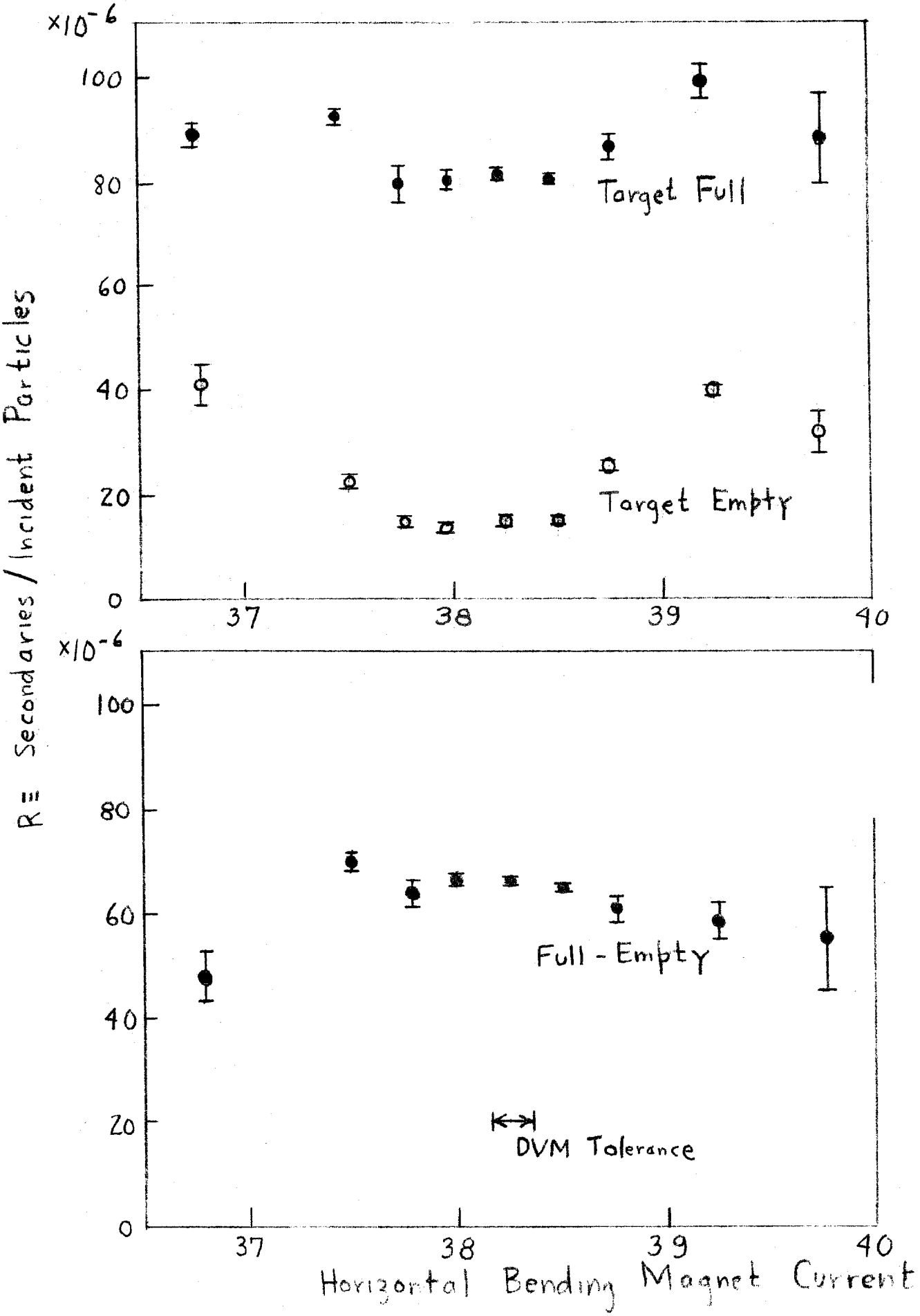
×10⁻⁶
100
80
60
40
20
0
37
38
39
40
Target Full
Target Empty
R = Secondaries / Incident Particles
×10⁻⁶
100
80
60
40
20
0
37
38
39
40
Full - Empty
DVM Tolerance
Horizontal Bending Magnet Current

Figure 3

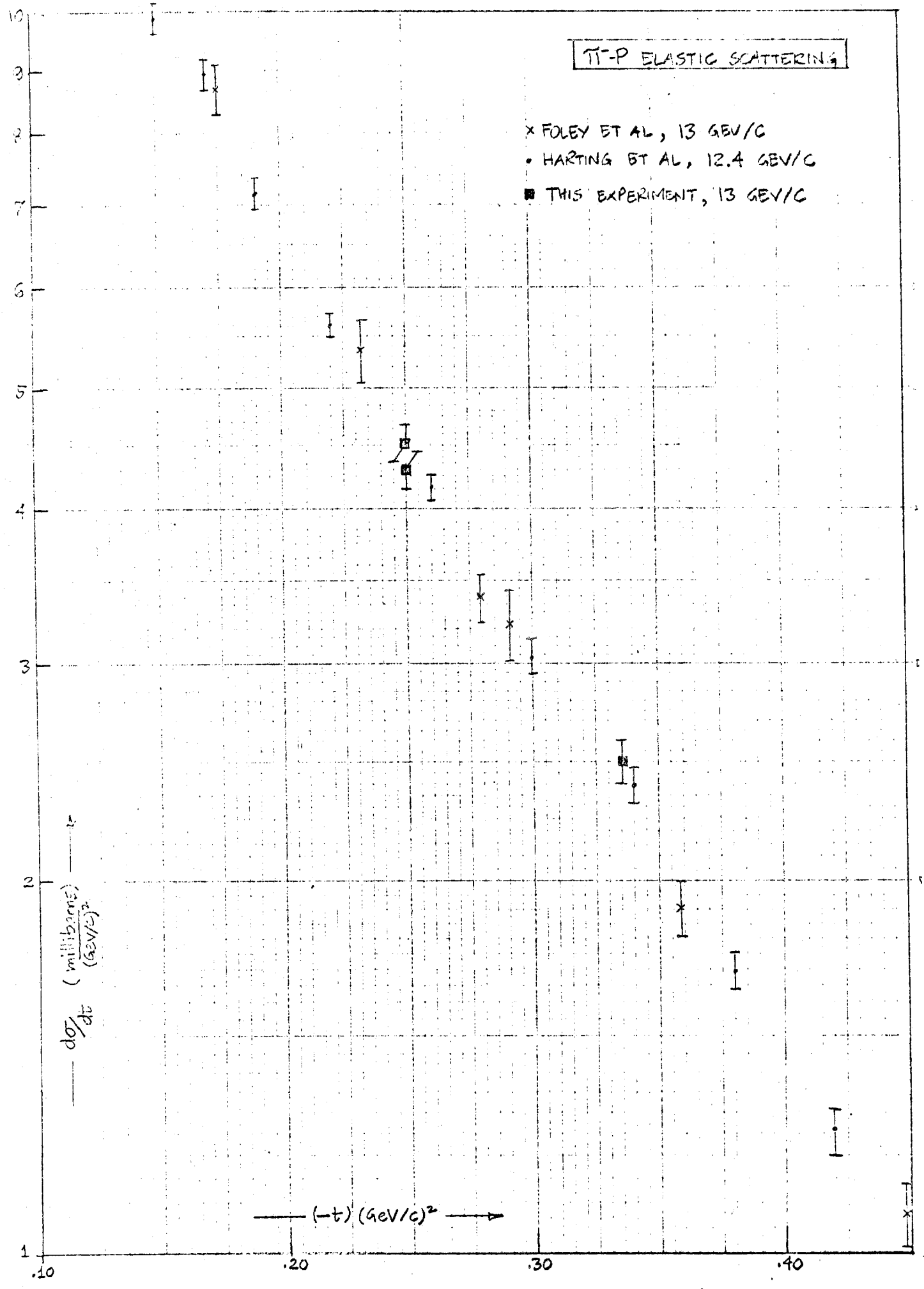
π^--P ELASTIC SCATTERING
× FOLEY ET AL, 13 GEV/C
• HARTING ET AL, 12.4 GEV/C
■ THIS EXPERIMENT, 13 GEV/C
$d\sigma/dt$ $\left(\frac{\text{millibarns}}{(\text{GeV/c})^2}\right)$
$(-t)$ $(\text{GeV/c})^2$
10
9
8
7
6
5
4
3
2
1
.10
.20
.30
.40

FIGURE 4

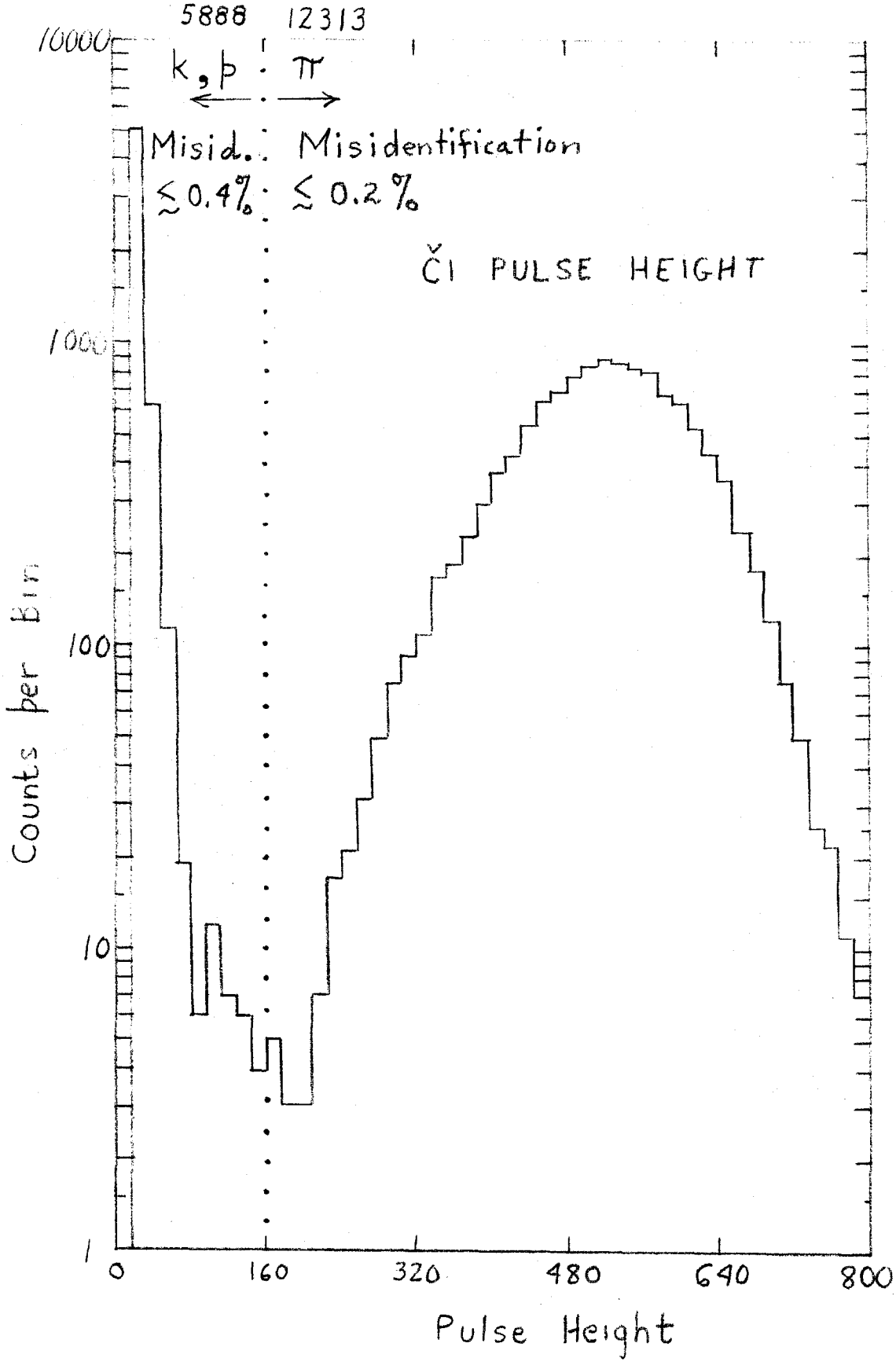
5888
12313
10000
K, p
π
Misid.
Misidentification
≲0.4%
≲0.2%
ČI PULSE HEIGHT
1000
100
10
1
Counts per Bin
0
160
320
480
640
800
Pulse Height

Figure 5a

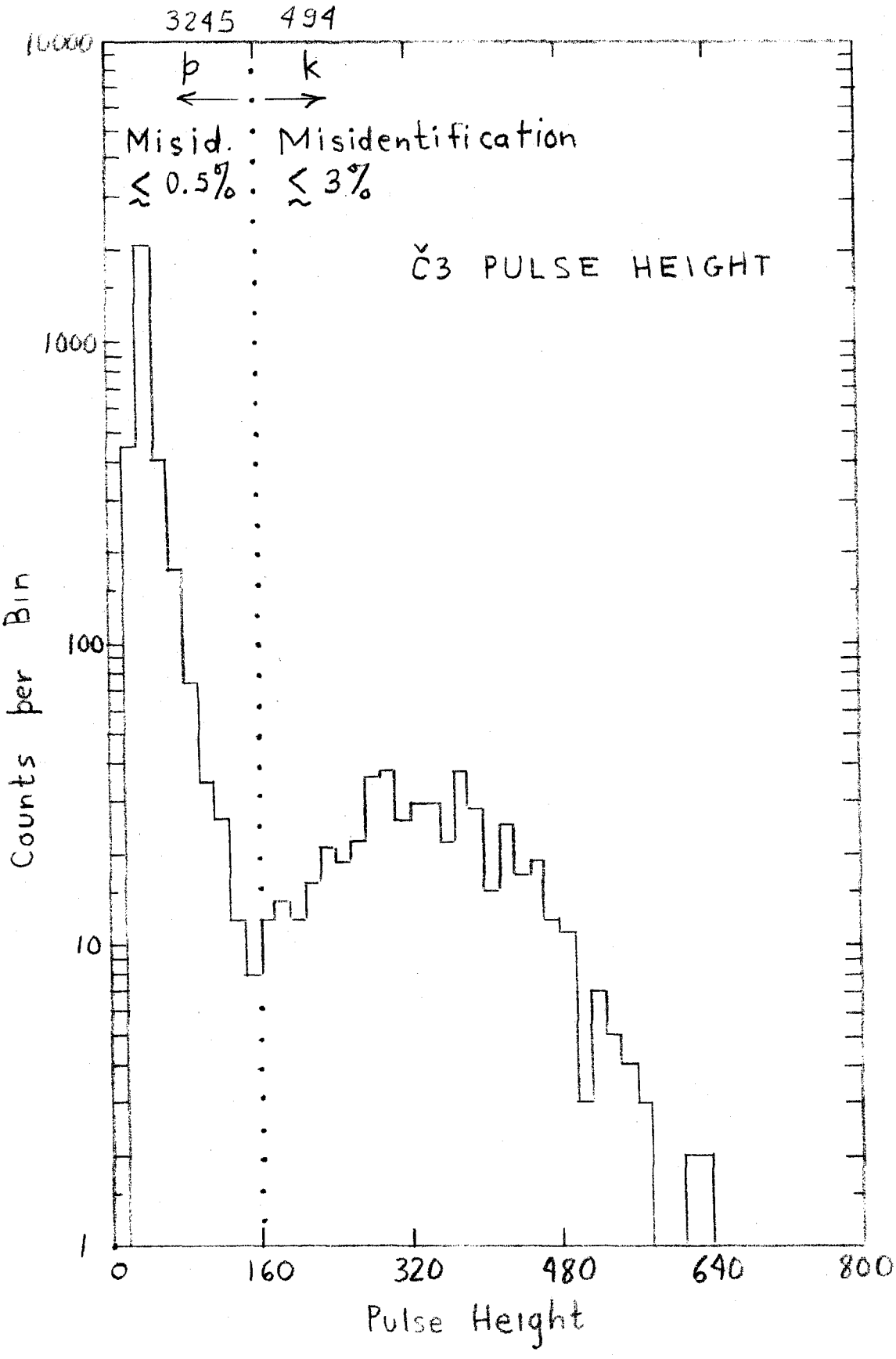
3245 494
10000
p
k
Misid. ≲ 0.5%
Misidentification ≲ 3%
Č3 PULSE HEIGHT
1000
100
10
1
Counts per Bin
0
160
320
480
640
800
Pulse Height

Figure 5b

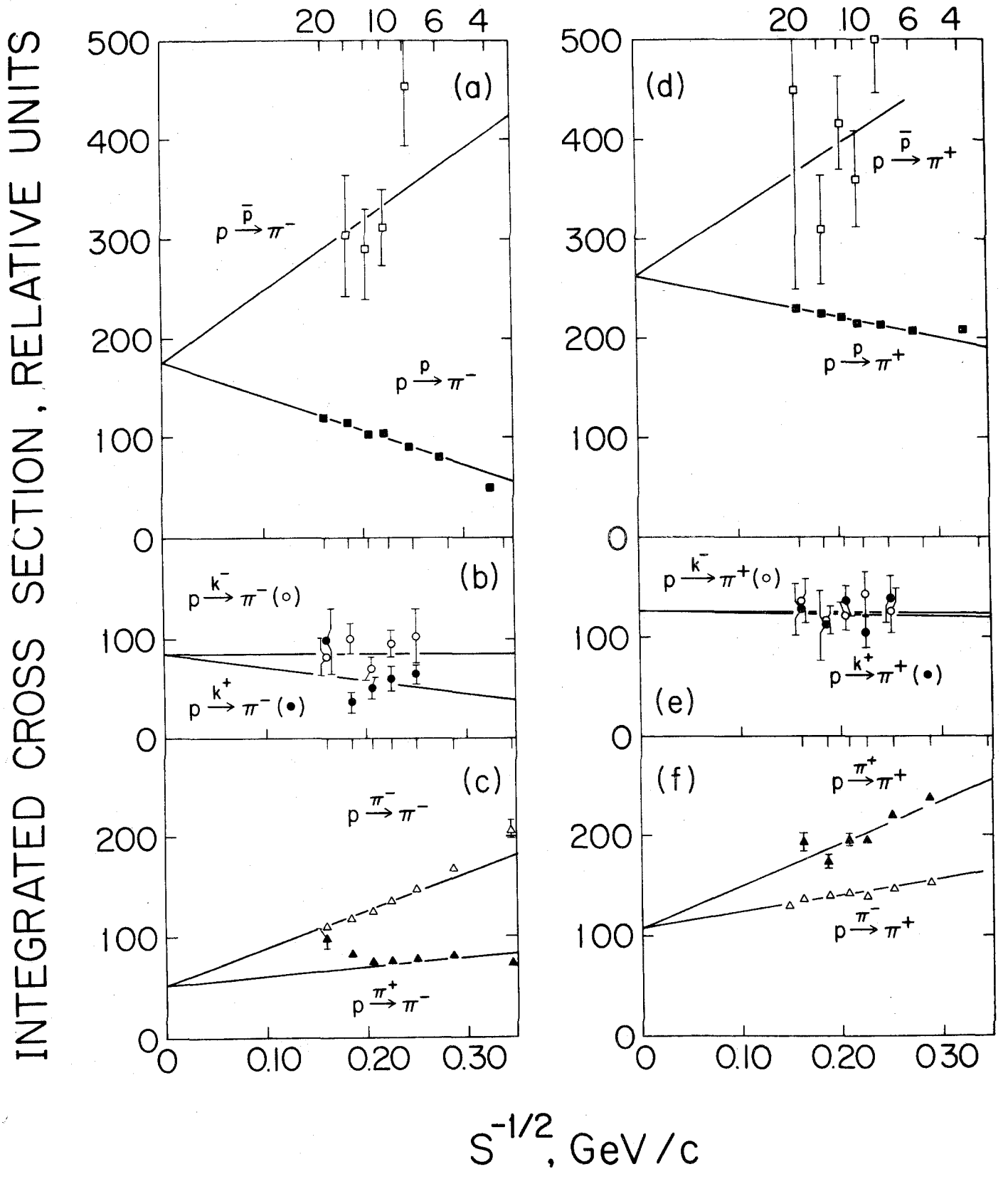
P beam , GeV/c
20 10 6 4
INTEGRATED CROSS SECTION, RELATIVE UNITS
500
400
300
200
100
0
(a)
p → π⁻
p → π⁻
(b)
p → π⁻ (○)
p → π⁻ (●)
(c)
p → π⁻
p → π⁻
0 0.10 0.20 0.30
(d)
p → π⁺
p → π⁺
(e)
p → π⁺(○)
p → π⁺ (●)
(f)
p → π⁺
p → π⁺
S^-1/2, GeV/c

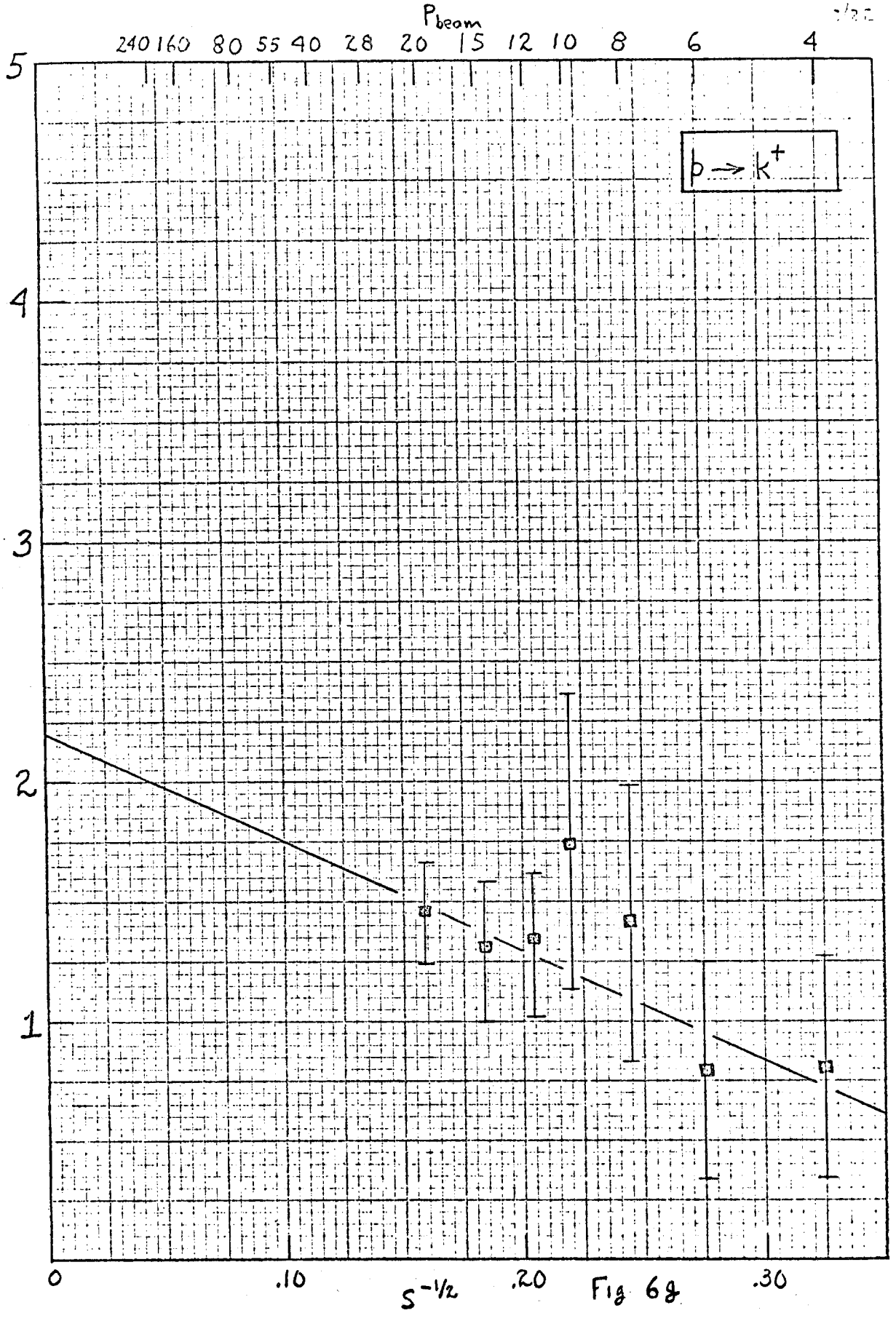

Fig 6g

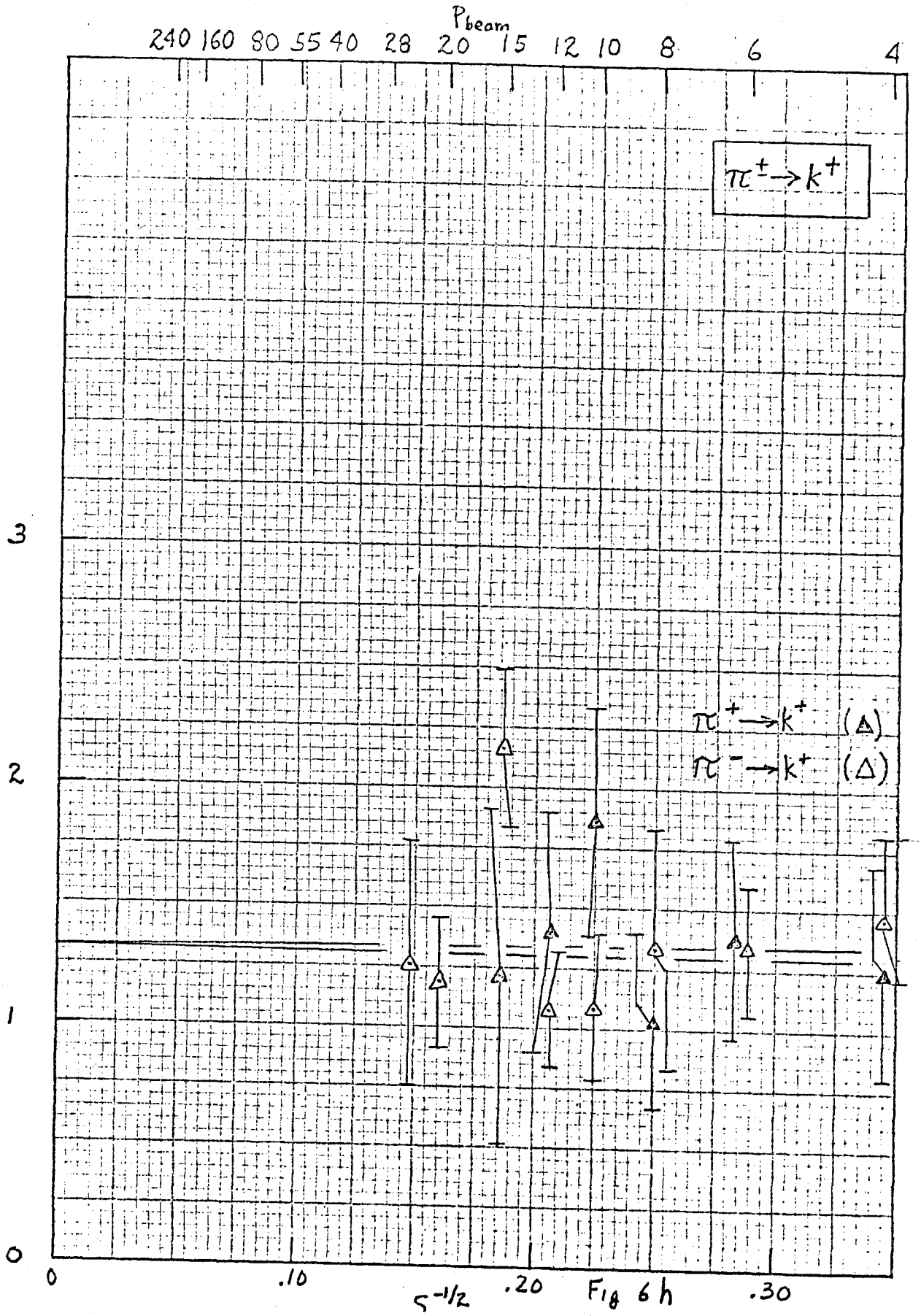
P_{beam}
240 160 80 55 40 28 20 15 12 10 8 6 4
$\pi^{\pm} \to k^{+}$
$\pi^{+} \to k^{+}$ (Δ)
$\pi^{-} \to k^{+}$ (Δ)
3
2
1
0
0
.10
.20
.30
$\varsigma^{-1/2}$

Fig 6h

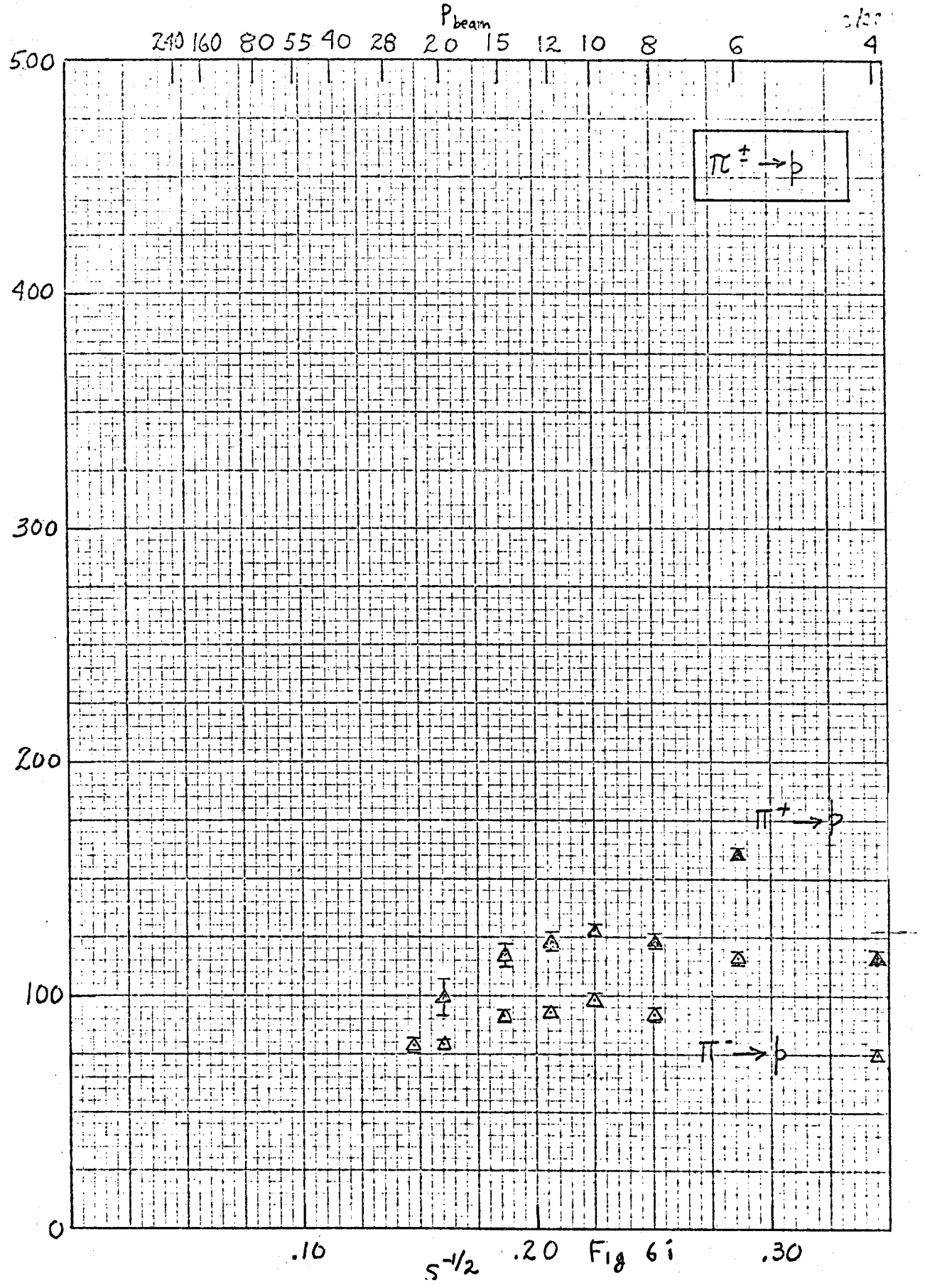
P_{beam}
240 160 80 55 40 28 20 15 12 10 8 6 4
500
400
300
200
100
0
$\pi^{\pm} \to p$
$\pi^+ \to p$
$\pi^- \to p$
.10
.20
.30
$s^{-1/2}$

Fig 6i

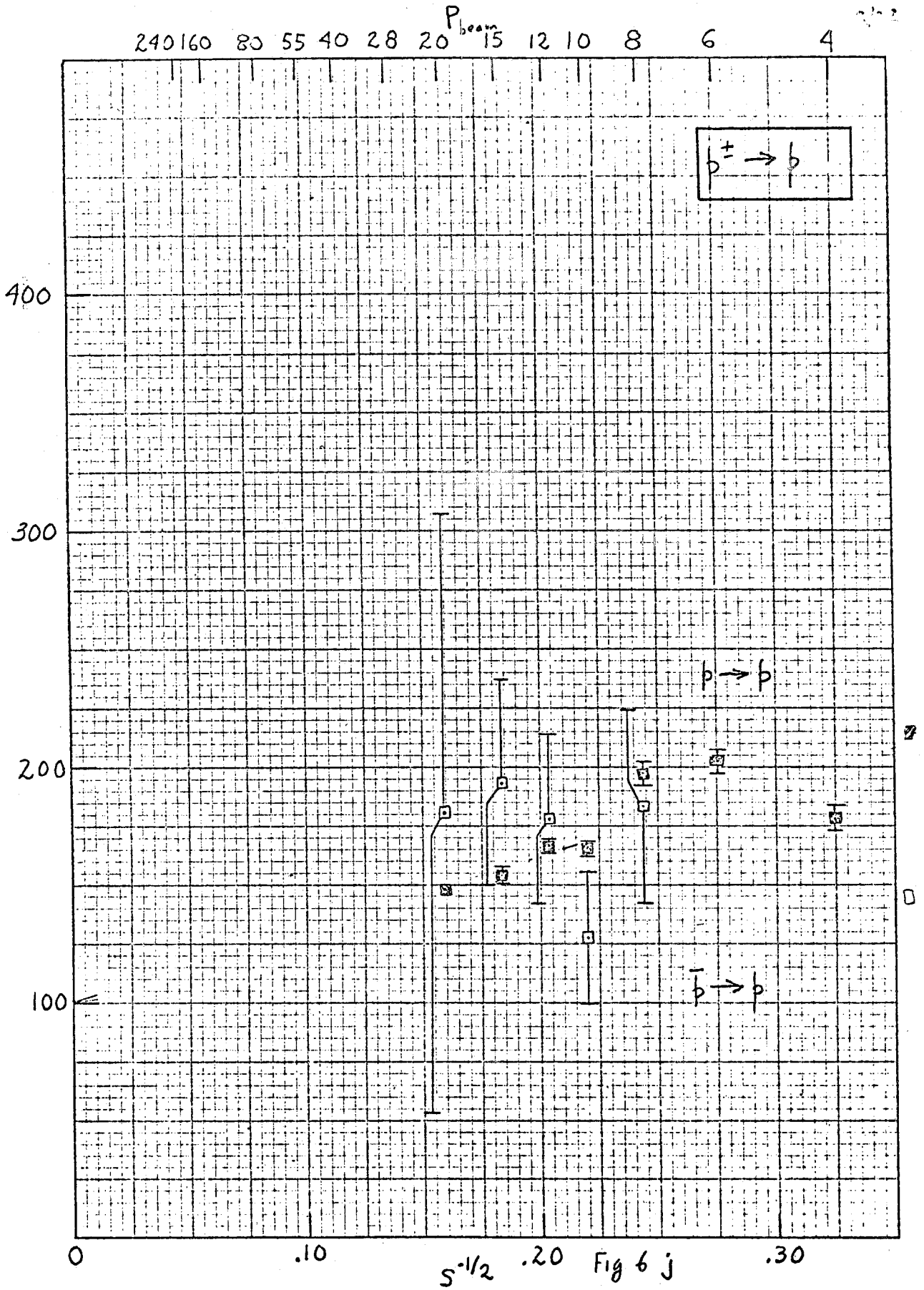
P_{beam}
240 160 80 55 40 28 20 15 12 10 8 6 4
$p^{\pm} \to p$
400
300
200
100
$p \to p$
$\bar{p} \to p$
0
.10
.20
.30
$s^{-1/2}$

Fig 6 j

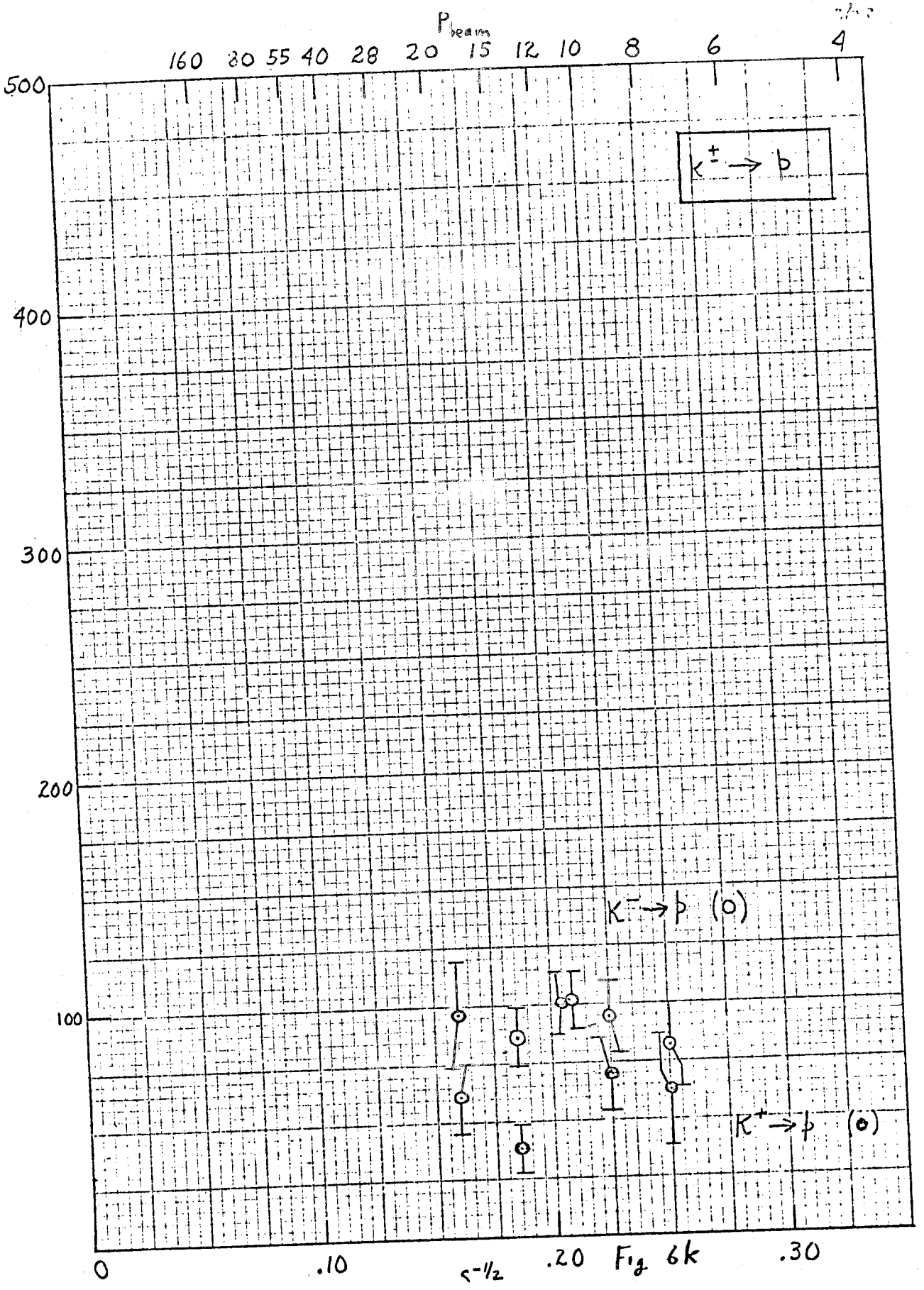
P_{beam}
160 80 55 40 28 20 15 12 10 8 6 4
500
400
300
200
100
0
.10
.20
.30
$K^{\pm} \to p$
$K^- \to p$ (○)
$K^+ \to p$ (●)
$<-1/2$

Fig 6k

ERRATA

Page 8, Paragraph 3, Line 2

... scattering, the behavior of which can .....

Page 18, Paragraph 2, Line 2

reaction ab→cd be

Page 30, Second line from bottom

.... beam rate to 0.3×10^{9} particles ...

Page 35, Paragraph 1, Line 11

.... the spectrometer length linearly with momentum ....